



Toward a dynamic concept of the subduction channel at erosive convergent margins with implications for interplate material transfer,

P. Vannucchi, F. Sage, J.M. Morgan, F. Remitti, J.Y. Collot

► To cite this version:

P. Vannucchi, F. Sage, J.M. Morgan, F. Remitti, J.Y. Collot. Toward a dynamic concept of the subduction channel at erosive convergent margins with implications for interplate material transfer,. Geochemistry, Geophysics, Geosystems, 2012, 13 (Q02003), pp.24. 10.1029/2011GC003846 . hal-00682642

HAL Id: hal-00682642

<https://hal.science/hal-00682642>

Submitted on 18 Mar 2022

HAL is a multi-disciplinary open access archive for the deposit and dissemination of scientific research documents, whether they are published or not. The documents may come from teaching and research institutions in France or abroad, or from public or private research centers.

L'archive ouverte pluridisciplinaire **HAL**, est destinée au dépôt et à la diffusion de documents scientifiques de niveau recherche, publiés ou non, émanant des établissements d'enseignement et de recherche français ou étrangers, des laboratoires publics ou privés.

Copyright



Toward a dynamic concept of the subduction channel at erosive convergent margins with implications for interplate material transfer

Paola Vannucchi

*Earth Science Department, University of Florence, Via La Pira 4, I-50121 Florence, Italy
(paola.vannucchi@unifi.it)*

Françoise Sage

*Géosciences Azur, Université Pierre et Marie Curie–Paris 6, BP 48, F-06235 Villefranche-sur-Mer
CEDEX, France*

Jason Phipps Morgan

*Department of Earth and Atmospheric Sciences, Cornell University, Snee Hall, Ithaca,
New York 14853-1504, USA*

Francesca Remitti

*Earth Science Department, University of Modena and Reggio Emilia, Largo S. Eufemia,
I-41100 Modena, Italy*

Jean-Yves Collot

*Géosciences Azur, Institut pour la Recherche et le Développement, BP 48,
F-06235 Villefranche-sur-Mer CEDEX, France*

[1] Convergent plate boundaries accommodate intraplate displacement within a ~100–1000 m thick shear zone. Marine geophysicists typically define this zone, the subduction channel (SC), as the sedimentary layer between the downgoing oceanic crust and the base of the upper plate. Geologists and modelers, instead, perceive the SC as a specific type of shear zone. The original theory of SCs was developed when the net accretion of marine sediments to the forearc was thought to typify a convergent margin. While erosive margins were briefly mentioned, their mechanics were not discussed in any detail. We now realize that subduction erosion is taking place at roughly half of the modern subduction margins. Here we review and revise the theory of erosive SCs (1) to unify this concept across disciplines, focusing on the meaning of the channel's boundaries; (2) to redefine the portions of the forearc included in the SC concept; and (3) to better idealize this dynamic system where material supply to the channel, fluid content, and the heterogeneity of deformation all influence the SC's upper and lower boundaries. Migration of the channel boundaries controls the downdip variation of tectonic mechanisms that shape the margin. Within the shallow, <15 km deep part of the SC, a gradual change of physical properties defines three zones; zone 1 of rapid fluid dewatering, zone 2 of overpressure, and zone 3 with metamorphic fluid release. A SC is a dynamic feature with along-strike and downdip variations caused by changes in channel material, in trapped fluid contents, and in interplate boundary geometry.

Components: 15,100 words, 8 figures.

Keywords: plate boundary; tectonic erosion.

Index Terms: 3060 Marine Geology and Geophysics: Subduction zone processes (1031, 3613, 8170, 8413); 8021 Structural Geology: Melanges; 8104 Tectonophysics: Continental margins: convergent.

Received 24 August 2011; **Revised** 4 January 2012; **Accepted** 7 January 2012; **Published** 10 February 2012.

Vannucchi, P., F. Sage, J. Phipps Morgan, F. Remitti, and J.-Y. Collot (2012), Toward a dynamic concept of the subduction channel at erosive convergent margins with implications for interplate material transfer, *Geochem. Geophys. Geosyst.*, **13**, Q02003, doi:10.1029/2011GC003846.

1. Introduction

[2] The overall mechanics of subduction zones have mainly been explored by two types of geodynamical models, the Coulomb wedge theory [Davis *et al.*, 1983; Dahlen *et al.*, 1984] and its modified dynamic version [Wang and Hu, 2006] and the SC model [Shreve and Cloos, 1986] (Figure 1).

[3] Coulomb wedge models are based entirely on brittle fracturing (Figure 1a). They are particularly useful because they consider the role of changing fluid pressure and strength coupled, by Wang and Hu [2006], with the subduction earthquake cycle. However, these models do not consider the role of temperature and the resulting oversimplified rheology limits their applicability at depths <15 km. Coulomb wedge theories typically idealize the décollement to be a single fault – although recent developments clearly recognize the limitations of this approximation for study of seismogenesis and plate interface dynamics [Wang, 2010].

[4] Geophysical and geological data have shown the décollement to be a special type of fault zone, characterized by a deformation zone of finite width. The subduction channel (SC) framework [Shreve and Cloos, 1986; Cloos and Shreve, 1988a, 1988b] better describes processes focused near and along the plate boundary (Figure 1b). The initial SC model envisioned shear deformation to be focused within a layer of poorly consolidated sediments sandwiched between two rigid plates [Cloos and Shreve, 1988a]. As incoming plate sediments approach the “strong” roof of the overriding plate, they undergo longitudinal compression. Material supply and the pattern of flow of this material is controlled by the ‘inlet’, or opening of the SC, which would control its capacity. The inlet was located at the foremost edge of the overriding plate basement at a distance of 10–20 km to ~50 km from the trench [Cloos and Shreve, 1988a] (Figure 1b). Physically, the Shreve and

Cloos inlet represents the leading edge of either forearc basement or the well-lithified inner portion of an accretionary prism. More recent observations have shown the roof of the ‘inlet’ is a dynamic edge that evolves with time. Furthermore, observations show the SC in the inlet region is much thinner, e.g., at most km-scale, than originally proposed.

[5] Either incoming plate or trench-fill sediment is the initial input into the SC. As material enters the channel, it flows downward (Figure 1b). If material supply exceeds channel removal, then the excess is offscraped, dewatered and transferred to the upper plate to form an accretionary prism. In the channel, sediments also dewater; those that consolidate near the roof can underplate to the forearc.

[6] The principal variables governing the flow in the channel are the pressure exerted by the hanging wall, the sediment’s relative buoyancy, sediment viscosity, and the shear rate across the channel. Material within the SC is usually modeled with a viscous rheology.

[7] The SC model has been extended to describe deeper geodynamic environments of subduction zones, and to explore the exhumation of ultra-high pressure rocks [England and Holland, 1979; Chopin, 1984, 2003; Ernst, 2006]. For example, Mancktelow [1995] and more recently Raimbourg and Kimura [2008] used a SC analytical solution to estimate high, non-lithostatic pressures (i.e., pressure deviations from mantle lithostatic pressure) in subduction zones.

[8] Although physically plausible, the original SC model has clear limitations and biases. For example, in Shreve and Cloos’s [1986] frontmost ‘zone of compression’, no SC was assumed to have yet formed (Figure 1). In contrast, geophysical investigations [Bangs *et al.*, 2004a; Sage *et al.*, 2006] and field studies [Vannucchi *et al.*, 2008] show that forearcs can develop a finite thickness SC directly at

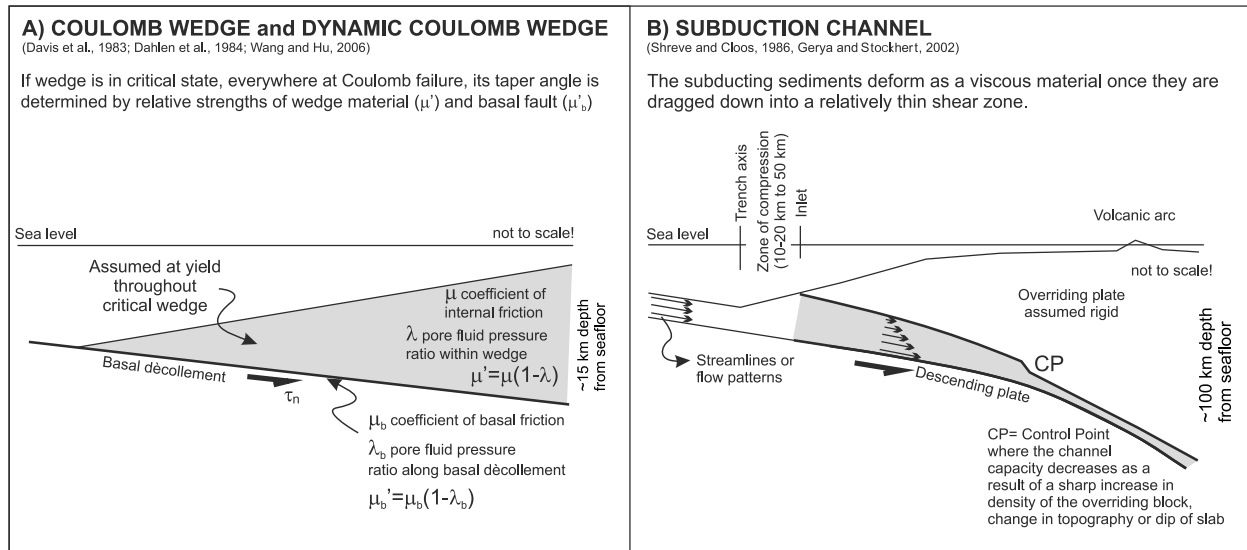


Figure 1. Cartoons summarizing the main characteristics of (a) the Coulomb wedge and Dynamic Coulomb wedge model and (b) the Subduction Channel model.

the frontal thrust, without a wide zone of near-trench compression in the forearc.

[9] The original SC model also assumed that sediment input into the channel would vary only when the trench sediment thickness and/or the convergence rate changed. Although subduction erosion was briefly mentioned, it was not actually modeled since the incoming plate was assumed to supply all channel material, while tectonically eroded material need not be incorporated at the channel inlet. Instead, an erosive plate boundary can incorporate either parts of the frontal prism or parts of the base of the upper plate or a mixture of both (Figure 2a) [Vannucchi et al., 2008; Wang et al., 2010]. Furthermore, oceanic and trench sediments vary in sedimentation rate and composition, which affects the accretionary or erosive nature, the compaction rate, and the width of the channel, in particular at accretionary systems (Figure 2b). Figure 2 shows geological material paths in two end-member – erosive and accretionary – SCs. This material can include (1) the sedimentary blanket on the incoming plate (for example, Figure 2b), (2) portions of seamounts/high relief structures on the incoming plate, (3) water-rich trench sediment supplied by along-slope mass-wasting and turbidites, (4) products of frontal and basal erosion that are gradually incorporated along the plate boundary (for example, Figure 2a).

[10] The assumed viscous rheology for channel material in the original SC model [Shreve and Cloos, 1986] implies a zero yield strength, while

plate boundary seismic events indicate there is a finite yield strength even at shallow (10–50 km) depths. Likewise, a viscous channel rheology would preclude localized shear zones with fault-like slip at both top and bottom boundaries, yet field studies on exhumed analogues of SCs [Kitamura et al., 2005; Vannucchi et al., 2008; Bachmann et al., 2009a, 2009b] and fine scale seismic interpretation of an active SC [Collot et al., 2011] show that both a basal shear zone and a principal roof shear zone coexist.

[11] Here we will focus in particular on the development of a SC at erosive margins, and will present a revised conceptual model for SCs consistent with these observations. We will introduce the concept of a dynamic SC that is active from the frontal thrust where the upper plate material and/or the incoming sediment pile starts to be affected by penetrative deformation. We also introduce a conceptual model that allows SC boundaries to migrate with time, implying its evolution in time and space. The model is inspired by field and seismic observations that directly provide constraints on the thickness of the interplate layer and the localization of shear deformation. Where appropriate we will use information obtained at accretionary margins to better constrain links between local fluid flow and local deformation processes. After discussing the observational foundation, we will reassess the key role played by the rate of sediment supply, the temporal and spatial variability of deformation mechanisms, and the depth and nature of subducted material. Our model most directly addresses the

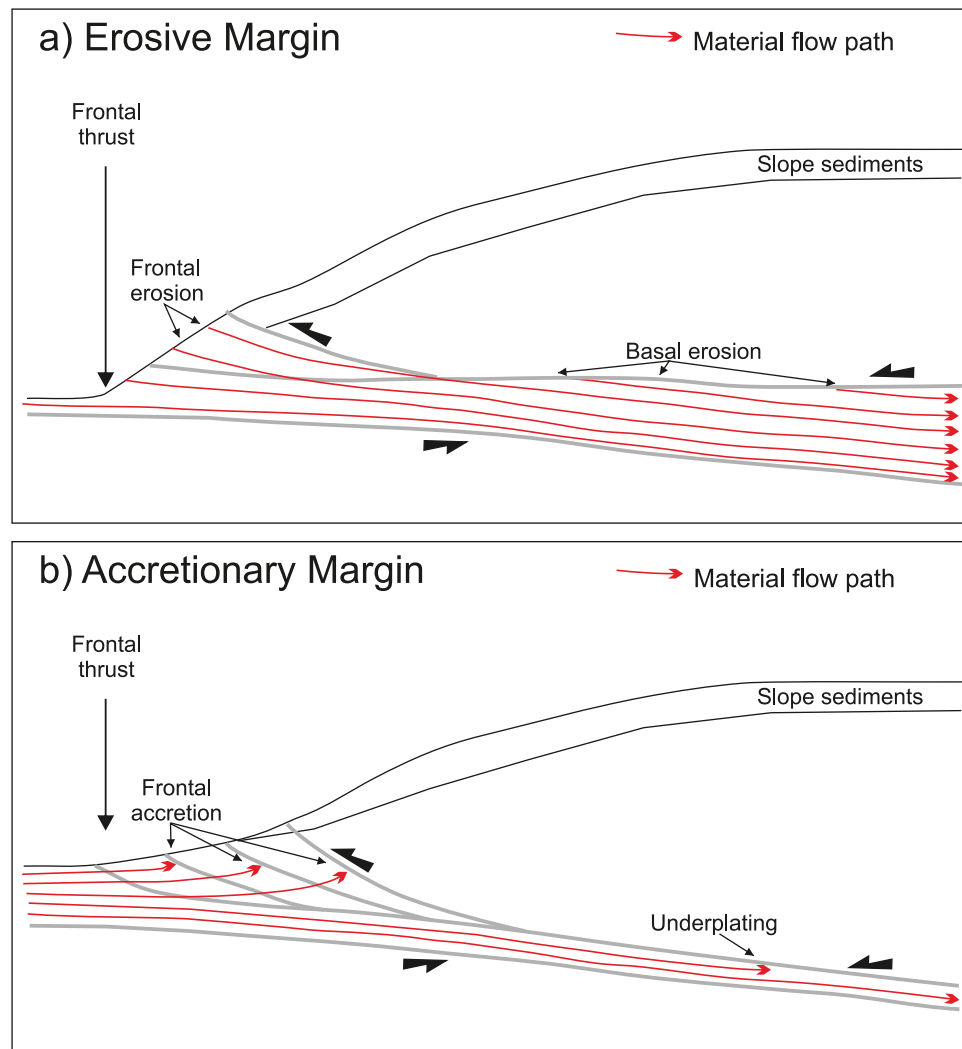


Figure 2. Cartoons showing the material flow paths for (a) an erosive and (b) an accretionary margin.

shallow portion of erosive subduction zones, i.e., <15 km depth, where geological and geophysical data are most abundant.

2. What Is a Subduction Channel? Seismic and the Field Study-Based Perspectives

[12] The SC has been perceived quite differently by geophysical, geological, and modeling communities. Geophysicists concentrate on discriminating the interplate layer from the surrounding upper and lower plate basements. Geologists and modelers focus on the zone where the shear deformation occurs, and the variability of deformation mechanism. These two approaches would be equivalent for *Shreve and Cloos's* [1986] SC where shear deformation is presumed to occur within unconsolidated,

high pore fluid pressure, viscous material sandwiched between stronger upper and lower plates. They may still match if we consider the subduction zone at a large scale as modelers do, especially in its deeper regions (depths >50 km). However, for shallower parts of the subduction zone (<~20 km depth), numerous recent geological and geophysical studies suggest that the relationships between the shear deformation zone and the interplate under-consolidated layer are more complex.

[13] Seismic images are interpreted to show the interplate sedimentary layer, which usually has remarkable density and seismic velocity contrasts with its surrounding upper and lower plate basement. This was originally inferred from low-resolution geophysical data [*Eberhart-Phillips and Reyners, 1999*]. In modern seismic images, this channel-like layer appears as a clearly defined low velocity zone

bounded at its top and bottom by bright reflectors; this zone can often be followed for several tens of kilometers landward of the trench [Tsuru *et al.*, 2002; Bangs *et al.*, 2004a; Calahorrano *et al.*, 2008; Bangs *et al.*, 2009; Tobin and Saffer, 2009]. Geophysicists often regard this interplate low-velocity layer as the SC [von Huene *et al.*, 2004; Calahorrano *et al.*, 2008; Collot *et al.*, 2008a; Ranero *et al.*, 2008; Scherwath *et al.*, 2010].

[14] However, seismic images support the idea that the shear deformation zone does not necessarily coincide with this interplate, low velocity, sedimentary layer. At the frontmost part of the subduction zone, incoming sediment remains undeformed below a weak décollement within its top section [von Huene and Scholl, 1991; Morgan and Karig, 1994; Housen *et al.*, 1996]. Downdip, relationships between the shear deformation zone and the interplate sedimentary layer become more complicated, especially where the accretionary or erosive nature and/or geometry of the plate boundary is complex. Local tectonic erosion and accretion probably contribute to the variability of the seismic images. Note that these two mechanisms can alternate both in time and space along a subduction zone. In accretionary SCs, material progressively lithifies, which at depth progressively minimizes the differences between overriding and subducting plates. In an erosive channel the material comes from the upper plate. In this case, the channel's top may have too small a velocity/impedance/density contrast to be resolved seismically. Ecuador provides a good example of the variability at erosive margins in the location of shear deformation with respect to the low-velocity interplate layer (Figure 3). Here, variations in thickness of the low velocity sedimentary interplate layer were explained to be due to episodic underthrusting of fluid-rich sediment supplied to the

trench by slope mass-wasting, and to subducting seamounts [Sage *et al.*, 2006]. This leads to strong patchiness within the interplate boundary, along which thick lenses of water-rich sediments alternate with thin drier segments (Figure 3). Above the interplate sedimentary lenses, the frontal part of the margin is uplifted, and normal faults cutting through the upper plate are rooted at the top of the interplate sediment layer (line SIS-12, Figure 3a). These geometries suggest that shear is not uniformly distributed across the low velocity interplate sedimentary layer, but instead is focused along its top. The shear zone is interpreted to be a weakly coupled décollement associated with overpressured fluids within the underthrust sediment (Figure 3a) [Sage *et al.*, 2006]. In contrast, where the SC is thin and dry (line SIS-64, Figure 3b), the presence of seaward-vergent thrusts at the margin basement's front implies higher interplate coupling. Landward of the thrusts, shear may distribute within a reflective zone where upper plate normal faults appear to root (Figure 3b). This reflective zone is interpreted as a damage zone at the base of the upper plate [Sage *et al.*, 2006]. The weakness of this damage zone, roughness at the top of the lower plate basement, and lack of a thick interplate sedimentary layer together suggest there may be distributed deformation over a thickness of ~ 800 m (Figure 3b). The thickness and geometry of the deformation zone vary considerably between these two Ecuadorian seismic lines which are separated by only a few kilometers (Figure 3c). This supports the idea that interplate heterogeneities control the location of zones of weakness along the plate interface.

[15] A hundred kilometers south of the seismic lines shown in Figure 3, the interpretation of recent high resolution seismic images shows that, in the subduction zone's shallowest 25 km, shear deformation

Figure 3. Pre-stack depth migrated multichannel seismic lines across the Ecuadorian subduction margin (modified from Sage *et al.* [2006]). (a) On line SIS-64, the interplate boundary is almost devoid of incoming sediment suggesting relatively high fault friction. Therefore, interplate deformation may be distributed over a few-hundreds-meters thick damage zone at the base of the upper plate. The damage zone is topped by a poorly defined roof thrust zone, and bounded at bottom by a clear undulating reflector interpreted to be the basal décollement. (b) On line SIS-12, a similar damage zone is observed along the base of the upper plate but is not considered to accommodate most present-day shortening. There, the interplate boundary shows an underthrusting low-velocity, fluid-rich lens of sediment. The rooting of basement normal faults at the top of the lens suggests that shear motion is mostly localized along the lens top. (c) Location of the seismic lines. (d) Schematic cartoon of the interplate boundary zone based on the above seismic images. The black lines at top delineate the low velocity interplate sedimentary layer interpreted as the subduction channel by seismologists. The black dash-dotted line at bottom follows the present interplate shear zone that would be interpreted as the subduction channel by geologists and modelers. Depending on local conditions such as the interplate geometry, fluid content, or the nature of the interplate sediment layer, shear deformation can either focus at the top of the interplate sedimentary layer (1), be distributed over the interplate sedimentary layer (2), or can involve part of the upper plate and/or lower plate basement (3). In these images, it is clear that the shear zone does not always coincide with the low velocity, interplate sedimentary layer.

localizes along faults within the interplate sediment layer [Collot *et al.*, 2011]. Here, the low velocity interplate layer is cut by oblique faults that we interpret as Riedel faults within a wider shear zone. The interplate layer is bounded by roof and basal thrusts [Collot *et al.*, 2011].

[16] Seismic images also provide strong arguments for the vertical migration of the interplate boundary

through time. Complex reflector patterns within the interplate layer indicate the downward migration of the plate boundary due to underplating of under-thrust sediments [Gutscher *et al.*, 1998; Park *et al.*, 2002; Collot *et al.*, 2008a, 2011]. Upward migration related to long-term basal erosion is demonstrated by truncation of reflectors of the upper plate at the top of the shear zone, and by normal faults

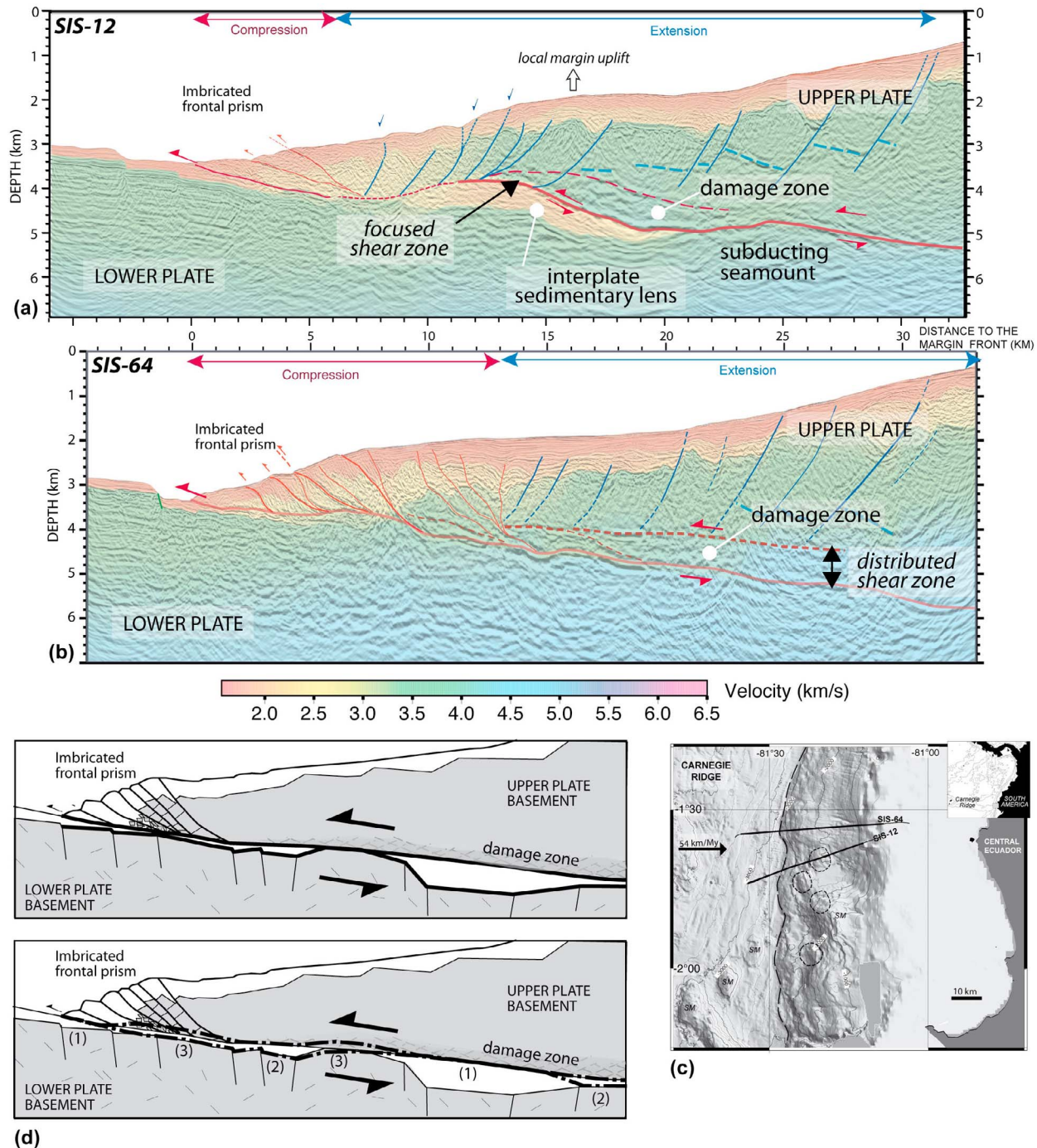


Figure 3

within the upper plate that accommodate subsidence above the removed material [von Huene and Lallemand, 1990; McIntosh et al., 1993; Klaeschen et al., 1994; Ranero and von Huene, 2000; Clift et al., 2003; Vannucchi et al., 2003]. Seismic data also show that basal erosion is enhanced where morphological asperities, like seamounts [von Huene et al., 2000], oceanic ridges [Hampel et al., 2004], or horst and graben systems [von Huene and Ranero, 2003] are observed at the top of the downgoing plate. The eroded fragments detached from the upper plate are subsequently incorporated to the interplate sedimentary layer [Ranero and von Huene, 2000].

[17] At accretionary margins, the locus of interplate shear deformation can vary through time, depending on the local dynamics of subduction. For example, along the Nankai accretionary prism, the interplate deformation zone shallows when deformation is transferred to a splay fault within the upper plate. This is associated with underthrusting at the décollement-splay fault junction of a thick section of material that was previously above the downgoing plate [Bangs et al., 2009].

[18] Seismic images also help in demonstrating the presence of fluids along the plate boundary. In particular, geophysicists interpret high reflectivity, especially when associated with negative polarity, as layers containing high-pressure fluids with large pore-volume fractions along the décollement [Collot et al., 2008b; Ranero et al., 2008; Ribodetti et al., 2011]. Reflectivity patterns indicate that fluid content decreases considerably at the updip limit of the seismogenic zone [Bangs et al., 2004b; Ranero et al., 2008]. Overpressured layers may be thin ($\ll 100$ m, too thin for seismic resolution), and irregularly distributed along the plate boundary interface [Bangs et al., 2004a, 2009; Ribodetti et al., 2011]. Furthermore, porosity values calculated from seismic velocities indicates that the underthrust sediment contains a large volume fraction of overpressured fluids [Sage et al., 2006; Calahorrano et al., 2008].

[19] Seismic methods have their limits. If the material in the channel does not have a significant difference in physical properties with respect to the upper and lower plate, then seismic imaging will not resolve it. Due to the low spatial resolution of seismic images at even a few kilometers depth, SCs thinner than ~ 200 m will not be properly resolved, even if they contain fluid-rich sediments thick enough to influence interplate deformation processes. Moreover, the low velocity inferred for the SC is an average value that does not account for

heterogeneities in smaller-scale fluid distribution. Overall, multichannel seismic imaging gives an instantaneous image of average fluid contents, and does not directly image variations in fluid distribution during a seismic cycle. Seismic imaging does not constrain the origin of the fluids. In conclusion, the low-velocity, seismically defined SC is too restrictive to embrace the whole range of processes affecting the interplate deformation zone.

[20] Field geologists take a different approach to SCs, focusing on deformation patterns as their defining characteristic. This definition requires that the overall motion of material in the interplate deformation zone is distinctive from the downgoing and overriding plates, regardless of the material's nature and origin. Study of fossil, now exhumed, subduction systems shows that the plate boundary is a fault zone of variable thickness where sediment subduction, mélange formation, and exhumation occur [Fisher and Byrne, 1987; Moore and Byrne, 1987; Hashimoto and Kimura, 1999; Ikesawa et al., 2005; Kitamura et al., 2005; Kondo et al., 2005; Federico et al., 2007; Vannucchi et al., 2008; Bachmann et al., 2009a, 2009b; Fagereng and Sibson, 2010]. The fossil SC outcropping in the Central Alps, for example, is represented by a mélange incorporating material either from the crystalline upper plate, or from the meta-ophiolites of the lower plate [Bachmann et al., 2009a, 2009b]. In the Shimanto belt in Japan, the fossil plate boundary zone consists of mélange packages incorporating shale-dominated and sandstone-dominated units that were underthrust beneath the offscraped accretionary prism to which they eventually underplated [Kitamura et al., 2005]. At the fossil erosive plate boundary in the Northern Apennines of Italy, the material incorporated in the SC all comes from the upper plate, none from the incoming plate sediments which remain undeformed beneath the basal décollement [Vannucchi et al., 2008]. The Apennine SC consists of blocks of (1) the overlying no-longer-active accretionary prism, (2) prism slope deposits, and (3) debris flows forming the frontal sedimentary prism [Vannucchi et al., 2008] (Figure 4). Here seismic images could probably not distinguish the active SC from underlying sediments, unless overpressured fluids generated a clear signal. The Apennine outcrops, moreover, show that deformation was both concentrated along the SC boundaries and distributed within the channel, as shear evolved along multiple surfaces parallel to those boundaries [Vannucchi et al., 2008, 2010].

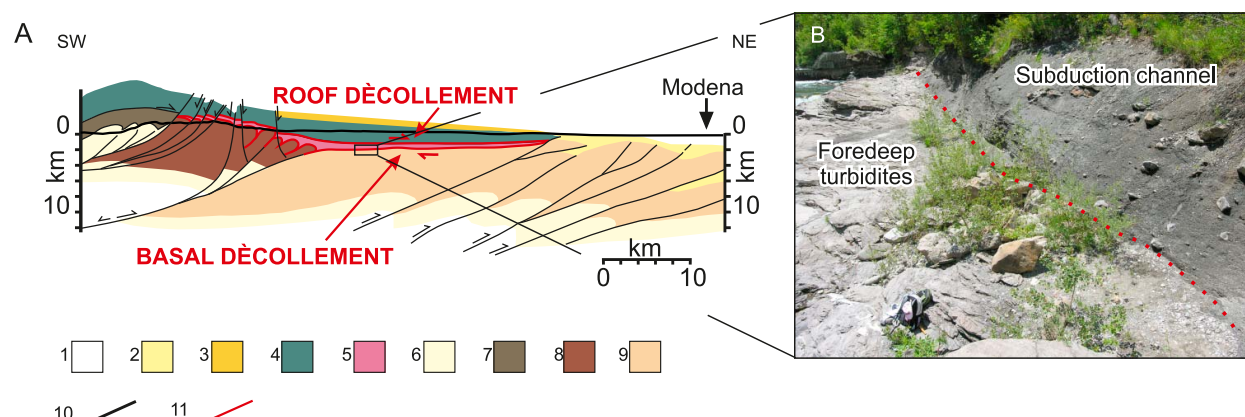


Figure 4. (a) Geological cross-section of the Northern Apennines subduction channel. Key: 1. Quaternary deposits; 2. Late Miocene-Pleistocene marine deposits; 3. Forearc slope deposits; 4. Oceanic units of the Late Cretaceous-early Eocene accretionary prism - European plate; 5. Sestola-Vidiciatico tectonic unit - Subduction channel; 6. Mesozoic carbonate units of the Adria plate; 7. late Oligocene- early Miocene (Aquitainian) trench turbidites of the Adria plate; 8. early Miocene (Aquitainian-Burdigalian) foredeep turbidites of the Adria plate; 9. middle Miocene-late Miocene (Langhian-Messinian) foredeep turbidites of the Adria plate; 10. Faults; 11. Subduction Channel boundary décollements. The thickness of the SVU is about 500 m slightly decreasing toward the NE. (b) Photograph of the basal decollement at Riolutato (Reggio Emilia).

[21] Field outcrops provide the opportunity to look at deformation structures and their evolution, for example, the stress transients recorded by some veins. Their mineral compositions also let us evaluate the nature of paleo-fluids. Drawbacks to field-based methods are that geologists look at patchy outcrops, and study material that may have changed its physical properties since it was deactivated and exhumed. Exhumation also allows surface processes to modify the upper plate topographic profile, create new sediment dispersal patterns, and superimpose new structures onto those present when the SC was active.

[22] Like field geologists, modelers use the SC to define the interplate boundary deformation zone with no intrinsic assumptions about the material's nature and origin [e.g., *Gerya and Stockhert, 2002*]. Although the physical properties (pore fluid, porosity, permeability) and rheology of the channel are difficult to estimate a priori, the concentration of deformation requires that the channel be weaker than its surrounding plates.

[23] From the geological and geophysical studies mentioned above, it is clear that in the shallower parts of the subduction system, shear deformation can localize anywhere within a broader megashear zone that potentially includes the low velocity layer, the base of the upper plate basement, and/or the top of the lower plate basement. This broad mega-shear zone may be viewed as the longterm SC, even if, at the scale of a seismic cycle, shear

further localizes depending on shorter-term physical and mechanical conditions. The mechanics and the deformation processes related to subduction zones cannot neglect the nature and rate(s) of sediment delivered to the SC, the heterogeneity of deformation along and within the plate boundary, and the downdip variation of tectonic mechanisms under conditions ranging from sediment dragdown to underplating. Nonetheless, the space-time variability in thickness and location of the shear zone relative to the soft layer is recognized by all three sub-disciplines.

[24] A key insight from these multiple observational approaches is that the SC can be described as a dynamic feature that varies in space and time along the same plate boundary. SC variation depends on local strength conditions that reflect the nature of the channel material, the amount of fluids present, and the interplate boundary geometry. This dynamic definition will be useful for illustrating and better understanding processes like basal erosion and underplating, earthquake nucleation, and slow and fast rupture propagation during seismogenesis.

3. Structure and Fluid State in the Shallow 0–15 km Section of Erosive Subduction Channels

[25] Data along modern and ancient subduction margins clearly shows a high fluid content at the

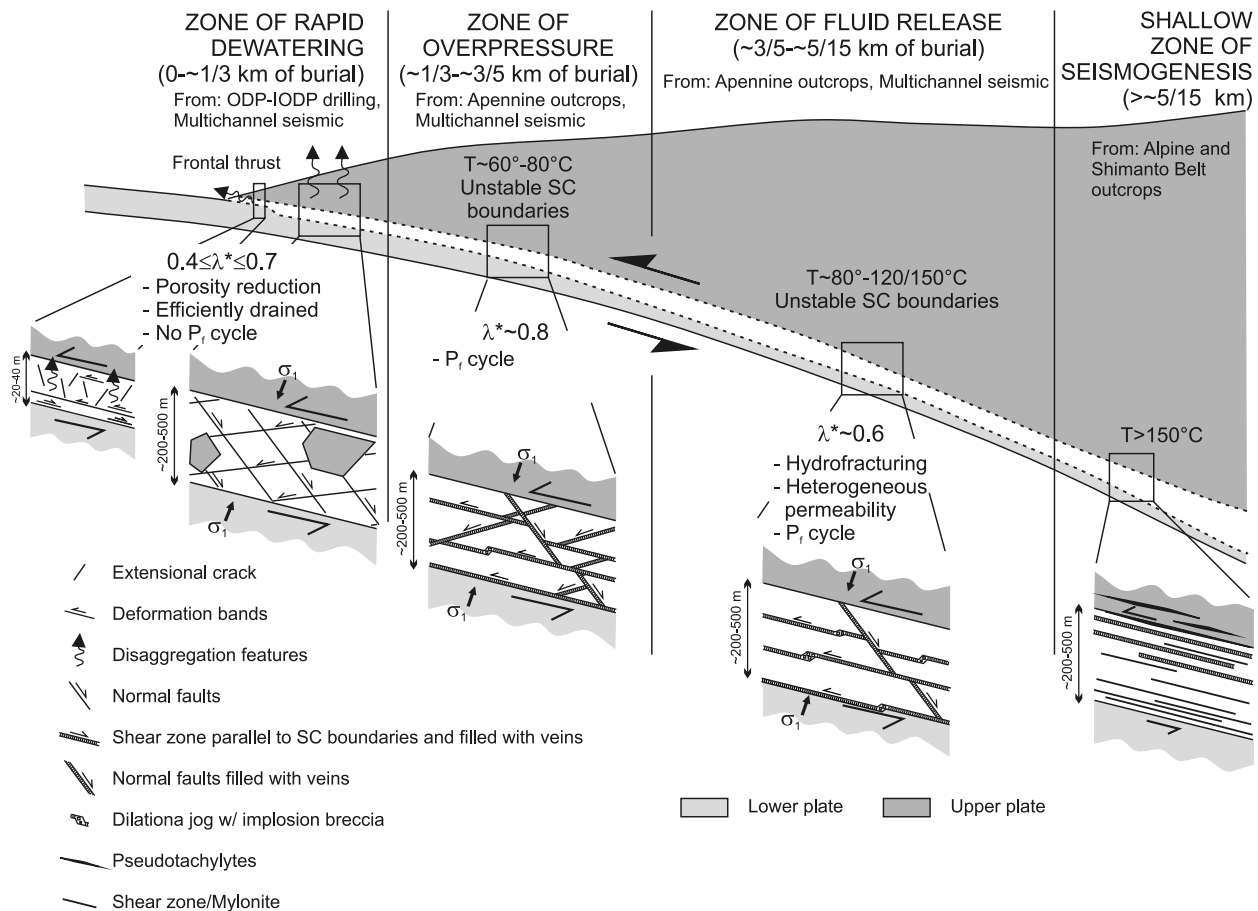


Figure 5. Cartoon showing the combined geophysical/geological characteristics of three different regimes (zones 1–3) of the subduction channel as the updip limit of megathrust seismogenesis is approached. Note that Zone 1 contains a strong change in thickness of the SC and evidence of reverse (Poisieulle-like) shear sense near the base of the SC.

interplate boundary. Fluids have effects on the mechanical and chemical disaggregation of the upper plate [von Huene *et al.*, 2004; Collot *et al.*, 2008a; Ranero *et al.*, 2008], on the frictional behavior of faults, and on rupture nucleation and propagation along the plate boundary [Mishra and Zhao, 2003; Moore and Lockner, 2004; Bangs *et al.*, 2009; Fagereng and Ellis, 2009; Wallace *et al.*, 2009]. The two main sources of fluid are (1) compaction of pore fluid-rich sediments and (2) metamorphic dehydration reactions in downgoing sediments and crust, and eventually in serpentinized lithospheric mantle at deeper sections of the plate boundary [Moore and Saffer, 2001; Rupke *et al.*, 2004; Vannucchi *et al.*, 2010]. Isotope analysis of carbonate veins in erosive SCs has also revealed the input of mineralizing fluids in equilibrium with eroded upper plate material [Vannucchi *et al.*, 2010].

[26] The fluid pressure regime and the fluid pathways in an erosive SC are key factors in controlling

material flow and the migration of SC boundaries. Data collected along ancient and modern subduction zones let us differentiate three main subsections of the SC above the updip limit of the ‘megathrust’ seismogenic zone (Figure 5).

[27] Zone 1: a shallow, fluid rich zone characterized by rapid dewatering at the front (from 0 to ~1–3 km of vertical burial). Here, fluid-rich/unlithified sediments are rapidly consolidating. There is diffuse extensional deformation of weak material and associated fluid migration – here fluid rapidly drains by both frontal and upward migration (Figure 5).

[28] The updip physical boundary of zone 1 is defined by the frontal thrust. The downdip limit of zone 1 is a diffuse boundary difficult to precisely characterize. Zone 1 extends downdip until the sediments in the channel are fairly well lithified. As channel sediments lithify, their deformation goes from diffuse to more localized, and they are able to

support episodic pressure buildups and drops [Calahorrano *et al.*, 2008; Vannucchi *et al.*, 2008].

[29] Seismic images of zone 1 show that V_P (seismic P-velocity) increases downdip, which is interpreted as a rapid reduction in porosity [Calahorrano *et al.*, 2008; Tsuji *et al.*, 2008]. This interpretation is based on the empirical V_P – porosity relationship [Erickson and Jarrard, 1998; Hoffman and Tobin, 2004; Raimbourg *et al.*, 2011] assuming that porosity exceeds the critical porosity f_c (~30%), defined as the transition between the suspension domain to the consolidated rock domain [Nur *et al.*, 1998]. At the Ecuadorian subduction zone, the porospace in zone 1 is calculated to decrease from 50% to 25% [Calahorrano *et al.*, 2008], which should lead to a major transition in the mechanical behavior of underthrust material. This seismic interpretation is supported by direct sampling of modern subduction zones drilled by the Ocean Drilling Program (ODP) and observations with submersible dives [Chamot-Rooke *et al.*, 1992; Collot *et al.*, 1992; Le Pichon *et al.*, 1992, 1994; Moore *et al.*, 1995; Kawamura *et al.*, 2009]. 50% porosity would imply that the medium is fluid supported at the margin front, and deformation is mainly dominated by grain rotation and frictional slip at grain contacts [Karner *et al.*, 2003]. The high porosity and high compactibility of incoming sediments promote fluid expulsion in response to the increasing load from overburden [Bolton *et al.*, 2000]. The calculated fluid overpressure ratio $\lambda^* = (P_f - P_{hyd}) / (P_{lit} - P_{hyd})$ is about 0.5 in zone 1 [Saffer and Bekins, 1998; Calahorrano *et al.*, 2008; Tsuji *et al.*, 2008]. Considering that $\lambda^* = 0$ corresponds to perfectly drained conditions and $\lambda^* = 1$ to full fluid retention, the calculated values suggest the presence of conduits that efficiently drain zone 1 so that fluid pressure remains sub-lithostatic. As the fluids are expelled, a significant part of the overburden load is transferred to the solid fraction of the underthrust material, and the mechanical behavior gradually changes to that of a consolidated media with a continuous solid matrix [Calahorrano *et al.*, 2008]. This mechanical change should significantly influence dewatering and deformation processes.

[30] Although incoming oceanic and trench sediments have >50% porosity, the SC contains a record of disaggregation features resulting from liquefaction and early onset of cementation and fracturing events [Vannucchi and Leoni, 2007] (Figure 5). Laboratory tests on the relationship between permeability and effective stress in Costa Rican fault zone samples show that shearing induces an

increase in bulk permeability that leads to rapid drainage and a consequent drop in fluid pressure [Bolton *et al.*, 2000], and also show that a small increase in effective stress can result in a significant volume of fluid expulsion [Saffer, 2003].

[31] Drillcores from Nankai Trough, Costa Rica, and Barbados indicate that the plate boundary is a brecciated horizon with a surface of concentrated slip usually located at the lower boundary or within this horizon [Maltman and Vannucchi, 2004; Vannucchi and Leoni, 2007]. The plate boundary is always a few tens of meters thick, even when it is <1 km from the trench [Maltman and Vannucchi, 2004]. Lithology and porosity seem to play a leading role in focusing shear, e.g., the region of shear is more concentrated in clayey layers than sandy layers. In general, brittle deformation, consisting of extensional and shear fractures, co-evolves with the fluid system (Figure 5). Feeble mineralization is observed along the fractures [Labaume *et al.*, 1997; Vannucchi and Leoni, 2007]. Geochemical data illustrate that the actual surface of concentrated slip is a somewhat permeable barrier to upward fluid flow with very little fluid passing across this zone; in contrast the adjacent brecciated part of the SC is a preferred conduit for fluid flow [Kimura *et al.*, 1997; Morris *et al.*, 2003; Sreaton and Saffer, 2005]. In Costa Rica, the upper part of the décollement zone is characterized by diffuse fracturing associated with dewatering and upward migration of fluids [Vannucchi and Leoni, 2007]. In these poorly consolidated sediments, only a small and localized overpressure is needed to trigger hydrofracturing. Hydrofracturing related to upward fluid migration may also lead to shallow and localized tectonic erosion [von Huene *et al.*, 2004].

[32] In the field, zone 1 (the zone of diffuse extension in the work of Vannucchi *et al.* [2008]) already shows well developed boundaries with basal and a roof surfaces of concentrated slip. These basal and roof décollements are easily detected in the field [Vannucchi *et al.*, 2008]. The roof décollement can migrate either by incorporating basal material from the forearc upper plate, or by incorporating frontal material from the toe of the forearc [von Huene *et al.*, 2004; Vannucchi *et al.*, 2008]. The basal décollement, instead, tends to focus shear deformation. It persists in a location where its shear strength is already minimized.

[33] Deformation is highly heterogeneous in zone 1. This is particularly visible in erosive SCs since they incorporate blocks of differently lithified

upper plate material. Here, episodes of typical pervasive extensional deformation do not cut through the rocks that already had been involved in previous upper plate deformation (Figure 5) – in the Apennine case a previous accretionary prism – and that were incorporated as well lithified, “rigid” blocks [Vannucchi *et al.*, 2008]. Instead, pervasive extensional deformation concentrates within sediments that were incorporated in the channel while still unlithified and weak. The Apennine pervasive extensional deformation indicates both failure and compaction in a fluid-rich environment [Vannucchi *et al.*, 2008]. The occurrence of a scale-independent network of very closely spaced fractures implies repeated failure. The fracture network has a high connectivity, implying an associated high permeability. Field exposures indicate a heterogeneous distribution of permeability and the occurrence of strong, undeformed blocks that, with less permeable layers, effectively work as local fluid barriers causing strong local variations in drainage. Fractures form without the intense calcite veining present in the deeper zones [Vannucchi *et al.*, 2008]. This lack of calcite vein mineralization can be related to the presence of low cohesion faults and shear fractures well oriented for frictional reactivation and preventing the formation of extensional or hybrid fractures where mineralization can occur [Sibson, 2001].

[34] The weakness of the deformed material that is undergoing continuous dewatering also implies the absence of a significant fluid pressure cycle – drainage occurred under quasi-stationary fluid pressure.

[35] Pervasive extensional deformation is recorded by a rhomb-shaped network of fractures that show a dominant tensional stress regime with a sub-vertical σ_1 . Extensional strain in the channel implies that the roof décollement behaved as a weak fault able to slip under a very misoriented (quasi-perpendicular) σ_1 , and able to transmit the lithostatic load to the channel. Recent interpretation of high-resolution multichannel seismic profiles in Ecuador indicates some high-angle, small throw normal faults/fracture (at a scale of ~ 100 m) [Collot *et al.*, 2010].

[36] In summary, the different data sets concur that the main deformation process in the frontal part of the SC is compaction that by itself could lead to high P_f , except that the porosity is so high and strength so low that high fluid overpressures cannot be maintained. A diffuse extensional fracture network efficiently moves fluids upward. This leads to progressive brecciation of the base of the upper plate for a few tens of meters as seen in Nankai and

Costa Rica [Maltman and Vannucchi, 2004]. The brecciated material forms the plate interface where it deforms, along with surfaces of localized slip, to accommodate plate convergence. The surfaces of localized slip seem to evolve from a system where only one surface is well developed – as in modern drilled margins – to a system where two slip surfaces form the boundaries of a SC.

[37] Zone 2: intermediate zone of overpressure (from ~ 1 –3 km to ~ 3 –5 km of vertical burial). This region is characterized by better consolidated sediments, discrete extensional deformation, the existence of high fluid pressures that rise well above hydrostatic pressure with the development of P_f cycles and associated vein precipitation, and preferential lateral migration of fluids within the higher permeability SC (Figure 5).

[38] Heat flow modeling along the erosive plate boundary offshore Costa Rica implies an ambient temperature of $\sim 60^\circ\text{C}$ to $\sim 80^\circ/100^\circ\text{C}$ for zone 2 [Grevemeyer *et al.*, 2004; Harris *et al.*, 2010a, 2010b]. Multichannel seismic reflection studies show high-amplitude reflectivity along the plate boundary fault, sometimes coupled with a negative polarity reflection [Ranero *et al.*, 2008]. This is also seen at accretionary margins [Bangs *et al.*, 2009]. High reflectivity can be associated with a large amount of fluids along the plate boundary [Ranero *et al.*, 2008; Bangs *et al.*, 2009]. However, in Ecuador the V_p along the “soft” interplate layer remains uniform [Sage *et al.*, 2006; Calahorrano *et al.*, 2008], with a porosity of $27 \pm 1\%$. This porosity value is high and surprisingly uniform over zone 2, in spite of increasing lithostatic pressure [Sage *et al.*, 2006; Calahorrano *et al.*, 2008]. The calculated fluid overpressure λ^* is ~ 0.8 [Saffer and Bekins, 1998; Calahorrano *et al.*, 2008]. Increasing forearc overburden is, therefore, in part compensated by an increasing fluid pressure within a SC [Calahorrano *et al.*, 2008]. These conditions favor hydrofracturing as a mechanism for fluid drainage.

[39] The interpretation of high-resolution multichannel seismic profiles in Ecuador suggests that in zone 2 there is a rhomb-shape fracture network very similar to the geometry described for zone 1 in the Apennines [Collot *et al.*, 2010]. Apennine outcrops of zone 2 show that normal faults and extensional fractures are still present, and that they cut through all components of the channel (Figure 5). Deformation occurred in more homogeneous and well lithified material in comparison to zone 1. Normal faults and extensional fractures occur here as frequently as do shear zones that parallel the channel’s

boundaries. Faults, fractures, and shear zones mutually crosscut, implying that during the opening of the extensional veins the shear surfaces were extremely weak [Vannucchi *et al.*, 2008; Fagereng *et al.*, 2010; Vannucchi *et al.*, 2010]. Many fractures also show characteristics of extensional, mode I failure. Macroscopic extensional veins, usually interpreted as the product of natural hydraulic fracturing, have special significance in that they require fluid pressure to have exceeded the least compressive stress ($P_f > \sigma_3$) with differential stress less than four times the tensile strength of the rock [$(\sigma_1 - \sigma_3) < 4T$] at the time of their formation [Secor, 1965].

[40] Zone 2 in the Apennine SC also shows widespread mineralization of faults and fractures by calcite veins. The mesh of mineralized fault and fractures can develop only in absence of well oriented, throughgoing cohesionless faults. Moreover the formation of extensional or shear-extensional fractures is favored by the presence of material characterized by high tensile strength [Sibson, 2000]. Therefore, not only the sediments in Zone 2 need to be lithified, but also fracture sealing by precipitation is necessary to build up transient high fluid pressure. The crack-seal structure of the calcite veins [Vannucchi *et al.*, 2010] suggests, following Ramsay [1980], that the mechanism responsible of the tensile fractures is hydraulic fracturing. During crack-seal a fluid filled open microfracture is formed which is later sealed through precipitation of crystalline material, calcite in this case. Calcium carbonate is coming from dissolution of the rock matrix through pressure solution and chemical transfer of this material in the low pressure, fluid filled space. Zone 2 also displays a few dilational jogs. These grow more abundant downdip to become a typical structure approaching the deeper zone 3.

[41] Hydrofracturing increases secondary porosity and possibly permeability, both competing with sealing by mineralization. The many preserved repeat episodes of hydrofracture suggests that this competition caused relatively ineffective drainage with persistent fluid overpressure in this portion of the channel. We interpret these observations to mean that, at the lengthscale of geophysical imaging, there is a net fluid overpressure, while smaller-scale outcrop observations show evidence of local hydrofracturing within this overpressured region. Such high fluid pressures have been suggested to weaken the base of the overriding plate, which would promote upward migration of the roof décollement and subduction erosion [von Huene *et al.*, 2004; Wang *et al.*, 2010].

[42] Stable isotope analyses of CaCO_3 in the veins of the Apennine SC show that mineralizing fluids come from three sources: downgoing sediment compaction, wallrock, and clay-mineral dehydration [Vannucchi *et al.*, 2010]. The partial overlap of vein isotope compositions with those of the wall-rock implies the occurrence of pressure-solution in the components of the SC that were eroded from the upper plate. The highest isotopic anomaly is recorded along the basal décollement. Here, $\delta^{18}\text{O}$ anomalies typical for clay mineral dehydration are present [Vannucchi *et al.*, 2010]. This dehydration process starts at temperature of $60^\circ\text{--}120^\circ\text{C}$ [Pytte and Reynolds, 1989; Moore and Vrolijk, 1992]. The basal décollement is a continuous shear zone that provided an effective pathway for transport of metamorphic fluids from depth [Vannucchi *et al.*, 2010]. This isotopic data indicates that zone 2 is primarily fed by fluids migrating updip from deeper portions of the channel.

[43] Fluids also migrate upwards toward the seafloor. In this case, thermal and geochemical characteristics of fluids sampled along vents of modern forearcs suggest that diagenetic reactions of clay minerals are the main fluid sources [Chan and Kastner, 2000; Moore and Saffer, 2001; Hensen *et al.*, 2004; Ranero *et al.*, 2008].

[44] The different data sets imply that zone 2 is characterized by a high fluid content and inefficient drainage that promotes fluid overpressure and persistent hydrofracturing. Compaction/lithification and overpressure appear to be linked to instability of the SC boundaries.

[45] Zone 3: deeper zone of fluid release (from $\sim 3\text{--}5$ to $\sim 5\text{--}15$ km of vertical burial). This region is characterized by complete consolidation and diagenesis of sediment, and the presence of overpressured fluids that effectively drain (Figure 5).

[46] Surface heat flow inferences indicate that zone 3 corresponds to a temperature range from $80^\circ/100^\circ\text{C}$ to $\sim 150^\circ\text{C}$ [Calahorra *et al.*, 2008; Ranero *et al.*, 2008]. These temperatures are near a threshold considered critical to trigger several processes more characteristic of the deeper seismogenic zone of the plate boundary. These processes are (1) the release of chemically bound water through metamorphic reactions, (2) the activation of pressure-solution diagenetic processes, and (3) the switch from aseismic to seismic strain release [Moore and Vrolijk, 1992; Moore and Saffer, 2001; Kitamura *et al.*, 2005; Bachmann *et al.*, 2009b; Kawabata *et al.*, 2009]. Thermal modeling of modern subduction zones suggests

that the updip limit of the seismogenic plate interface corresponds to temperatures around 100°C to 150°C [Hyndman *et al.*, 1997; Oleskevich *et al.*, 1999; Moore and Saffer, 2001; Newman *et al.*, 2002; Obana *et al.*, 2003; Currie *et al.*, 2004; Ranero *et al.*, 2008]. Recently Marcaillou *et al.* [2008] proposed an even lower temperature, 60°C, for the updip seismogenic limit of the Colombian margin.

[47] Multichannel seismic data image the updip limit of the seismogenic zone to be the transition from a strongly reflective to a weakly reflective plate boundary [Ranero *et al.*, 2008]. Geophysical modeling indicates that in this transition zone the porosity drops to ~10%, while the fluid overpressure ratio decreases to values of $\lambda^* < 0.6$, which leads to an increase in effective stress [Calahorrano *et al.*, 2008]. These observations suggest that pore fluids are being more effectively expelled so that the system is relatively well drained. Geochemical evidence from both pore water collected on the shallow, zone 1 of modern subduction zones, and veins collected along fossil plate boundaries indicates that there is lateral migration of these fluids along the SC [Silver *et al.*, 2000; Vannucchi *et al.*, 2010]. Drainage along the SC is possible because it is controlled by the fluid pressure gradient, rather than the relative fluid overpressure, so deeper fluids will tend to migrate into zone 2 as long as their P_f is higher than that in zone 2. These deep fluids also feed surface seeps, especially when splay faults serve as conduits through the forearc [Henry *et al.*, 2002]. This implies partial migration of fluid through the upper plate to the seafloor [Hensen *et al.*, 2004].

[48] In Apennine outcrops, slip planes cut through all lithological components in zone 3, indicating the frictional properties of this material are relatively homogeneous, consistent with a region of now-complete lithification of the slope sediment component of the SC. Like zone 2, the field expression of zone 3 shows evidence for hydrofracturing and P_f cycles. If the mineralized faults and fractures are geometrically arranged as in zones 1–2, the spacing of structures increases from ~1 m in zone 1 to >10 m here. Hence, the distribution of hydrofracturing-induced permeability is more localized and focused. We infer that drainage was efficient enough to relax fluid overpressures over this lengthscale.

[49] In the Apennines record, dilational jogs are key features of this portion of the SC. Jogs are characterized by the occurrence of implosion breccias

[Vannucchi *et al.*, 2010]. Dilational jogs filled by implosion breccias have been related to rupture associated with slip along a fault [Okamoto *et al.*, 2006]. Moreover, preserved dilational jogs have been related to seismogenic behavior of fault systems under conditions of high fluid pressure [Micklethwaite and Cox, 2006].

[50] In summary, zone 3 of erosive SCs contains abundant fluids that trigger hydrofractures able to efficiently drain the system. Structures are present which indicate there is a well developed P_f cycle associated with episodic slip along weak planes — e.g., this region contains the onset of the seismic behavior of the SC. Moreover, porosity reduction by compaction has reduced the volume of the material reaching this portion of the channel by ~50%; the fluids released by this compaction try to exit the channel. As discussed below, this effect can lead to a non-simple shear component of flow (dynamic flow) within this weak SC, which here could be the main cause of instability of the channel's upper and lower boundaries.

[51] Zone 4: updip limit of the seismogenic zone (between 5 and 15 km of burial). This region is characterized by seismic stress release, increasing metamorphism, and relative high fluid pressure (Figure 5).

[52] The updip limit of the seismogenic zone is not a sharp boundary, and the seismogenic zone forms a large portion of the plate boundary between the overriding crust and downgoing slab. Here the mechanisms of deformation change with increasing pressure and temperature conditions. We will focus only on the upper part of the seismogenic portion of the SC, i.e., regions with $T < 200^\circ\text{C}$ [Hyndman *et al.*, 1997; Moore and Saffer, 2001; Obana *et al.*, 2003; Ranero *et al.*, 2008]. Multichannel seismic data do not document a standard pattern of reflectivity variations for ~100–150°C plate interfaces. In South Colombia-North Ecuador as well as in Cascadia the plate interface becomes reflective at depths greater than ~10 km where the subduction thrust is inferred to be locked [Nedimović *et al.*, 2003; Collot *et al.*, 2008a]. In Costa Rica and Nankai, at these depths the reflectivity abruptly decreases, which is interpreted to reflect a change to a drier fault [Bangs *et al.*, 2004a; Ranero *et al.*, 2008]. Following this idea, grain-to-grain contact should increase with depth as water escapes, causing the effective normal stress across the plate-boundary fault and seismic coupling to increase [Scholz, 1998]. Calahorrano *et al.* [2008]

proposed a scenario where the supercritical compaction of sediment [Karner *et al.*, 2003] could lead to a macroscopic yield stage where cataclasis induces an acceleration of compaction and a general collapse of the system [Wong *et al.*, 1997].

[53] However, this appealing idea of a dry fault is disproved by field data that show that seismic SCs were fluid rich. The Apennine field example only touches the conditions described for the seismogenic SC, being associated with a maximum temperature of about 120–150°C. Here mineralization is always well developed along all exposures [Vannucchi *et al.*, 2010]. Evidence for elevated fluid pressure around the roof décollement has been reported from several outcropping SCs [Kitamura *et al.*, 2005; Bachmann *et al.*, 2009b]. In the Shimanto Belt, mineralized veins and cementation are associated with pseudotachylytes along the roof décollement of a sediment-dominated SC in a temperature range around 180°C to 200°C [Ikesawa *et al.*, 2005; Kitamura *et al.*, 2005]. This indicates fault zone fluid-saturation during repeated deformation, likely between seismic events, and maybe even during a seismic event [Okamoto *et al.*, 2006; Ujiie *et al.*, 2007]. In the Central Alps, a SC ranging from 150°C to 350°C is also characterized by extensional fractures and shear zones that evolve into mylonites at depth, with abundant evidence for pressure-solution [Bachmann *et al.*, 2009a, 2009b]. There, in an interval corresponding to temperatures between 200°C–300°C, pseudotachylytes are found. They are restricted to the upper plate crystalline rocks in mutual association with vein systems, indicating that rapid failure occurred in the SC. Both these examples reveal that (1) key mechanical and kinematic role for the roof décollement as the predominant shear zone, (2) fluid flow supports apparently mutually exclusive processes such as long-term interseismic deformation (solution-precipitation creep, mylonitization of pseudotachylytes) and short-term coseismic deformation (fracturing) and pseudotachylytes, (3) the presence of sealed compartments of the SC that develop transient lithostatic fluid pressures in association with cyclic deformation (the seismic cycle), and (4) that the seismogenic zone of SCs sustains seismic rupture regardless of its hydraulic state.

[54] Both modern and fossil SCs have features indicating that their seismogenic zone has a heterogeneous pressure distribution. Compartments of high fluid pressure can be areas of hydrofracturing at the base of the upper plate in which basal tectonic erosion is concentrated [von Huene *et al.*, 2004; Calahorrano *et al.*, 2008]. Upward migration,

though, seems to be more limited than it is in zone 1, because in general there is a high permeability contrast across the roof décollement. Fluid drainage can locally increase frictional strength, which could induce downstepping of the roof décollement, and hence underplating. At the Ecuador-Colombia margin, for example, the locked zone, at a depth of ~14–15 km and *T* of ~120°–140°C, becomes the locus of underplating, likely in a close geometric relation with an overlying forearc splay fault system [Collot *et al.*, 2008a].

[55] In moving from the toe to the seismogenic zone, the focus of deformation seems to migrate from the basal décollement in zone 1 to the roof décollement in zones 3 and 4. In zone 1, differences in the original compositions and porosity of sediments can control the localization of shear. Shear would focus toward the base of the channel while fluids tend to migrate upward, and successfully drain. As the deeper parts of the channel are approached, fluid concentration appears to become the main cause of low strength along the basal décollement.

4. The Dynamic Subduction Channel

[56] SC sediments were initially idealized to be constant density, uniform viscosity, and with a permeability depending only on porosity [Shreve and Cloos, 1986]. From the geological data summarized above we know that the viscosity, density and permeability of channel sediments vary not only along strike and downdip, but also throughout the channel itself. Viscosity, for example, varies as a function of both lithology and the degree of lithification. Bedding anisotropy, large unconformities, lithification and variable pore fluid pressure produce heterogeneities that can strongly influence flow in the channel. For example, sediments entering the SC have different degrees of lithification, and deformation tends to concentrate in poorly lithified, weaker horizons. These horizons can be alternating depositional layers, or chaotically arranged blocks, either as mélanges or as hard rock blocks dislodged from the upper or lower plate and incorporated in the channel [Fagereng and Sibson, 2010]. In these cases, while some components have a brittle behavior, others deform viscoplastically [Vannucchi *et al.*, 2010]. Since the degree of lithification depends strongly on depth, fluid pressure, and rock type, this parameter most likely differs between margins, and within each margin it can vary downdip, along strike and throughout the channel.

[57] Heterogeneous material properties implies a flow pattern where different components travel at different velocities within the channel (Figure 6a). In a uniform viscous rheology, shear is partitioned uniformly across the channel and material pathways are represented as flow lines that parallel the channel boundaries [Shreve and Cloos, 1986] (Figure 6b). However, field observations show that shear can be localized on multiple simultaneously active adjacent fault zones, implying non-viscous rheology at a local scale (Figure 6c) [Vannucchi et al., 2008; Fagereng and Sibson, 2010]. Rheological effects from the progressive dewatering and consolidation of channel material (Figure 6d) will be discussed in the next paragraph. Although the velocity cross-section (the velocity profile across any given section of the channel) can be smooth or inhomogeneous, material is typically envisioned as flowing in smoothly varying layers (Figure 6a). Nonetheless, material heterogeneity, as well as geometric variations along the channel, can induce velocity changes that can result in flow break-up into a more complex pattern of larger layer structure “currents” mixed with short order “chaos.” In the rock record, examples of these various kinds of flow are represented by “mesoscopic” tectonic mélanges [Fisher and Byrne, 1987; Moore and Byrne, 1987; Meneghini et al., 2010], “map-scale” tectonic mélanges, [Vannucchi et al., 2008] and SCs formed by “coherent” units detached along tabular fault zones [Remitti et al., 2011]. The variation from smooth to chaotic flow can produce morphologies ranging from anastomosing and bifurcating shear zones to the chaotic deformation typical of mélanges. Flow variations are also associated with local variations in channel thickness.

[58] Material flow in the channel occurs by both discrete transient slip surfaces and distributed creep [Vannucchi et al., 2009]. Considering that different strain mechanisms like viscous creep, tremor, and slow slip events all occur in forearcs; material flow occurs though these combined processes repeated thousands of times.

[59] Geological observations also imply that sediments have a strong fracture permeability, even at shallow depths, in addition to their pore-permeability. Ocean drilling at Costa Rica and Nankai, for example, revealed that the décollement is represented by a tens of meters thick brecciated horizon [Maltman and Vannucchi, 2004] (Figure 5). Geochemical studies of modern décollements and fossil exhumed examples show that fluids mostly circulating through fractures [Morris et al., 2003; Vannucchi et al., 2010].

Transient fluid overpressures and hydrofracturing seem to commonly occur in the shallower parts of SCs [Vannucchi and Leoni, 2007].

[60] The following dynamic model of the SC considers the frontal thrust, a m-scale-thick fault at ODP site 170–1043, as the leading edge, or top to the seafloor inlet of the SC. The migration of the channel boundaries, or roof and basal décollements, are key factors shaping input and output to the channel. There are eight basic geometries for the migration of the décollements (Figure 7).

[61] An example dynamic SC is represented by the Ecuadorian margin (Figure 3). Line SIS-64 is interpreted to show a zone of distributed shear within the upper plate damage zone, considered to be the weakest region along the plate boundary [Sage et al., 2006]. The damage zone is inferred to be bounded at top by a poorly defined roof thrust zone and at bottom by the top of the downgoing plate. Here the weaker region of the plate boundary is the basal décollement at the base of the damage zone (Figure 3). On line SIS-12 a similar damage zone is observed at the bottom of the upper plate, but above a low-velocity fluid-rich sediment lens. Here, the geometric characteristics imply that shear focuses along a décollement at the base of the damage zone. In this case, the more highly pressurized décollement would be weaker than the less pressurized damage zone [Sage et al., 2006].

[62] Vertical migration of the SC boundaries could also control the rheology of the channel. Upward migration of the roof décollement at the front, or downward migration of the basal décollement in the incoming and lower plate would result in incorporation of weak, yet to be lithified material into the channel. The subducting plate’s drainage conditions, and its capability to release fluids, also depends strongly on the nature of the underthrust sediments [Townend, 1997; Sibson and Rowland, 2003]. A stiffer channel rheology would result from the incorporation of upper plate material by basal tectonic erosion or by removal of material from the lower plate at considerable depth. This heterogeneous material would have variable mechanical characteristics (e.g., porosity, Young modulus, etc.), and a variable response to in situ stress and fluid pressure changes, with consequences for fluid connectivity and drainage.

[63] Décollement migration determines the occurrence of subduction accretion and/or erosion. Accretion and erosion, in fact, are processes that do not mutually exclude each other in time and

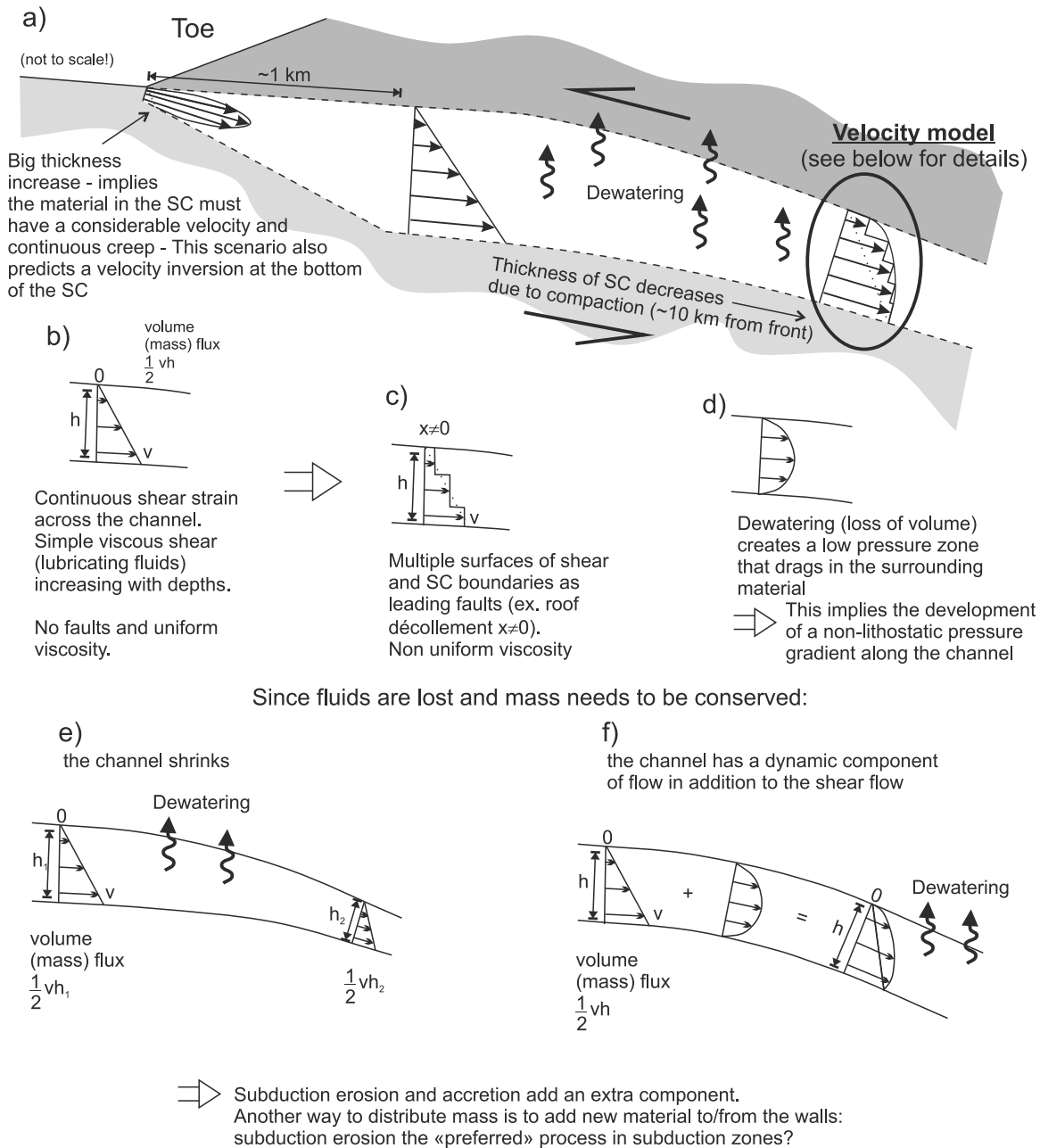
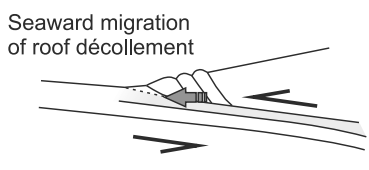
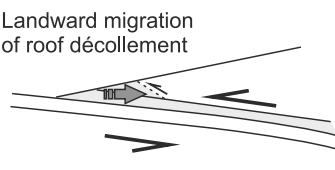
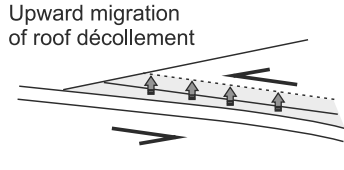
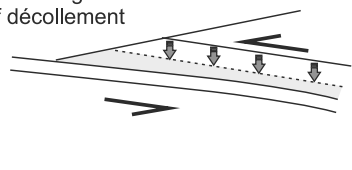


Figure 6. Illustration of the deformation patterns that occur within the subduction channel. (a) Potential large-scale patterns of material flow within the upper regions of the subduction channel. At the toe the subduction channel has a relatively small thickness that rapidly increases (see text). This is consistent with the toe having rapid flow of extremely fluid and poorly consolidated material (see text). Further downdip, compaction of material in the channel can induce both channel shrinkage (Figure 6e) and a component of dynamic flow (Figure 6f). (b) Sketch of the distributed shear occurring within a purely viscous channel rheology. (c) Sketch of deformation pattern when multiple local shear surfaces remain active within the subduction channel. (d) Sketch of potential viscous deformation component associated with a non-lithostatic pressure gradient within the channel. Note that this component of deformation requires a finite-width channel (as opposed to a thin fault zone) in order to become a significant component of material transport. (e) Channel shrinkage can compensate volume loss due to fluid escape. (f) In addition, dynamic flow within the channel can compensate volume loss due to fluid escape. If the channel remains quasi-uniform in thickness while undergoing a significant loss of pore fluid, then this mode of deformation must be happening within the channel.

Migration of roof décollement:

<p>1) Seaward=Frontal accretion</p>  <p>Seaward migration of roof décollement</p> <p>new material would be added to the upper plate through frontal accretion</p>	<p>2) Landward=Frontal erosion</p>  <p>Landward migration of roof décollement</p> <p>upper plate material would enter the subduction channel from the front resulting in frontal tectonic erosion</p>
<p>3) Upward=Basal erosion</p>  <p>Upward migration of roof décollement</p> <p>new material is added to the subduction channel with the result being tectonic erosion of the upper plate, and addition of new material to the channel.</p>	<p>4) Downward=Underplating</p>  <p>Downward migration of roof décollement</p> <p>material is removed from the channel and accreted to the upper plate through underplating.</p>

Migration of basal décollement:

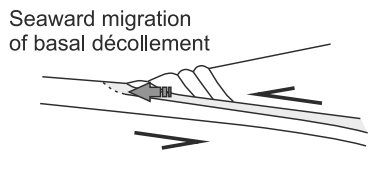
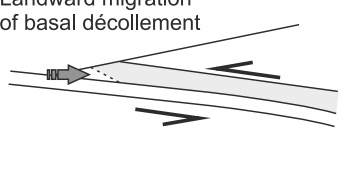
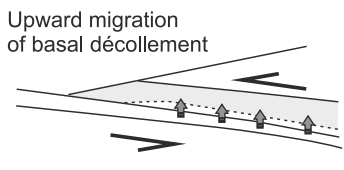
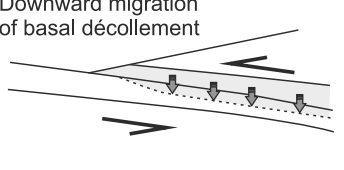
<p>5) Seaward=Offscraping</p>  <p>Seaward migration of basal décollement</p> <p>new material would be offscraped and added to the subduction channel</p>	<p>6) Landward</p>  <p>Landward migration of basal décollement</p> <p>subduction channel material would be added to the subducting plate</p>
<p>7) Upward=Erosion of SC</p>  <p>Upward migration of basal décollement</p> <p>material of the subduction channel is added to the subducting plate. In this case there is erosion of the subduction channel.</p>	<p>8) Downward=Accretion to the SC</p>  <p>Downward migration of basal décollement</p> <p>new material would be added to the subduction channel: at the front this would result in offscraping.</p>

Figure 7. Cartoons of the possible migrations of the roof and basal décollements and associated effects on the tectonic processes shaping the margin.

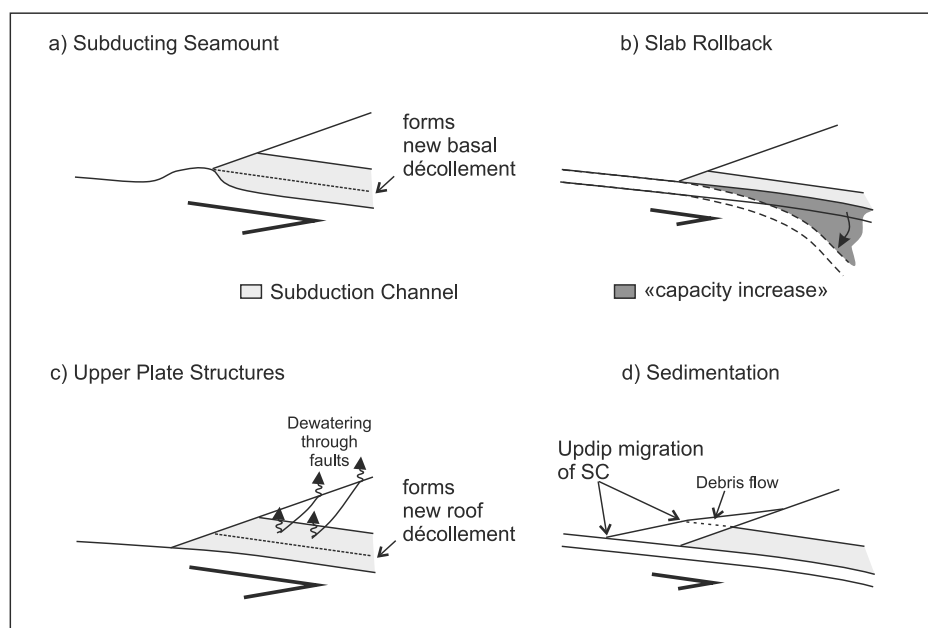


Figure 8. Examples of possible migration patterns of the subduction channel boundaries in response to some common events that occur at subduction zones: (a) a subducting seamount, (b) slab rollback, (c) development or reactivation of inherited structures cutting through the upper plate, and (d) rapid change of sedimentation rate in the trench (for example, mass wasting).

space – i.e., they simultaneously occur along different downdip and along-strike portions of the Ecuadoran plate margin [Collot *et al.*, 2008b].

[64] Décollement migration can be controlled by a number of factors, including the following:

[65] 1. The morphology of the incoming plate (Figure 8a). Structural highs such as seamounts and ridges, and related lows on the incoming plate can deflect the roof and basal décollements [Cloos and Shreve, 1996; Dominguez *et al.*, 1998, 2000]. Even if highly localized, it will still contribute to along-strike variations in deformation mechanism and SC geometry. A well-lithified subducting seamount, for example, has been found to cause landward and upward migration of the basal décollement [Dominguez *et al.*, 1998]. If the height of the seamount is greater than the thickness of the channel, then locally the roof décollement must migrate upwards. This could result in large tectonic erosion of the frontal margin, as at the Bougainville Seamount in the New Hebrides [Collot *et al.*, 1992] or the Cocos plate seamounts in Costa Rica [von Huene *et al.*, 2004]. In the wake of the subducting seamount, a large shadow zone can develop, with collapse of portions of the weakened upper plate into the channel.

[66] 2. The geometry of the slab (Figure 8b). Roll-back (i.e., the tendency of a subducting plate to

retreat from the trench/foredeep, and the opposite prograde motion of the subducting plate toward the overriding plate) may strongly influence the shallow dip of the slab. If the upper plate does not keep moving seaward at the same speed as the retreating slab, this would progressively increase the volume of material entering the SC. In other words changes in the dip of the slab/décollement could force the thickness of the channel to increase, especially in its deeper portions, and also force the upper décollement to migrate.

[67] 3. Upper plate dynamics (Figure 8c). Sedimentation, surface erosion and the deformation style of the upper plate can influence décollement migration. Multichannel seismic studies of the Nankai accretionary prism have been interpreted to indicate an upper décollement downstep and underplating where a major forearc structural discontinuity, the so-called splay fault [Park *et al.*, 2002], joins the SC [Kimura *et al.*, 1997; Bangs *et al.*, 2004a]. The Nankai roof décollement downstep was linked to a change in fluid pressure and increase of frictional strength of the décollement induced by the preferential dewatering pathway represented by the splay fault [Kimura *et al.*, 1997; Strasser *et al.*, 2009]. The preferred interpretation of more recent 3D imaging is that there is a downstep from a now inactive décollement at this juncture [Strasser *et al.*, 2009; Kimura *et al.*, 2011].

[68] In contrast, landslides would change the load and the profile of the upper plate slope, which would influence the state of stress at the décollement. Landslides would also cause material to accumulate at the trench, as discussed below.

[69] 4. Subduction speed and sediment supply (Figure 8d). Worldwide patterns suggest that accretionary prisms preferentially grow in margins where slow convergence (<7.6 cm/yr) and/or high trench sediment thickness (>1 km) occur [Clift and Vannucchi, 2004]. The opposite pattern characterizes erosive margins. Cause-effect relationships are not easy to disentangle in this context because of interference from surface processes, such as onland erosion, that control the volume of sediment delivered to the trench, with deeper processes, such as slab pull, that could affect the convergence rate [Clift and Vannucchi, 2004]. A slow convergence rate, for example, would allow more time for clastic trench sedimentation to occur. The big sediment pile at the trench can simply be frontally accreted, if the inlet capacity does not allow an increasing volume of material to enter the SC. The formation of a frontal accretionary prism would force the SC to propagate seaward. But since sediments also retain a large amount of fluids, trench sedimentation would also influence pore pressure evolution, fluid release and the mechanical stability of the SC.

[70] 5. Fluids. Fluids are lubricants, but also key factors in controlling cementation, dynamic processes within faults, and the rheology of the SC. Consolidation and upward migration of fluids can deactivate the basal décollement, and weaken the upper part of the SC with respect to the bottom, which could favor upward migration of the roof décollement [von Huene et al., 2004]. On the other hand, a sudden dewatering event in the channel such as the transient opening of a fluid pathway represented by a slipping fault, could drain the upper part of the SC increasing its cohesion and so induce underplating of this dewatered channel material.

5. Implications for Geodynamic Modeling

[71] What does this revised scenario imply for the development of future, more complete, models of subduction dynamics? A first order implication is the reaffirmation that subduction plate boundaries are deformation zones with a finite width as proposed by Shreve and Cloos [1986], not single faults. The processes controlling this remain poorly understood

because the yield strength of channel and forearc material is so heterogeneous and process-dependent. Several examples in both modern [Bangs et al., 2004a; Sage et al., 2006; Calahorrano et al., 2008; Wallace et al., 2009; Collot et al., 2010] and fossil analogues [Kitamura et al., 2005; Vannucchi et al., 2008; Bachmann et al., 2009a, 2009b] show that the preferred channel width is typically a few tens to hundreds of meters. A width comparison between modern and fossil systems involves the deciphering of fossil compaction. Fluids almost certainly play a key role in processes regulating material input and output into the SC. Fluids influence the material's shear strength, and are a key mobile component within the channel. Fluid release through compaction and metamorphic dehydration reactions contributes to changes in the volume of the material in the channel – it causes progressive material escape in the form of highly mobile fluids. If uncompensated, this would cause a continuous reduction of the SC thickness with depth. As a consequence the SC is compactible. This observed behavior has interesting implications. Figure 6 starts from Shreve and Cloos's [1986] scenario for an idealized SC filled with uniform viscosity, incompressible, sediments. In this case, shear stress is continuous across the channel, the velocity increases uniformly across the channel, and faults would not develop. Compaction and fluid dewatering implies net volume loss from channel material (Figure 6d). Downdip reconstructions of SCs remain sparse [Calahorrano et al., 2008; Bachmann et al., 2009b], but they indicate changes in width/thickness with depth. A compactible version of Shreve and Cloos's [1986] shearflow model would predict a continual decrease of the channel thickness with depth due, for example, to sediment compaction during dewatering. (Note that, for an idealized viscous fluid, this postulated downdip thinning of the channel would be associated with a proportional increase in the shear stress transmitted across the channel. The inclusion of more complex constitutive equations can also lead to non-lithostatic pressure variations [Raimbourg and Kimura, 2008].) More generally, downdip changes in channel thickness would need to be accommodated by deformation within its overlying and underlying regions. Dewatering-induced compaction within a weak channel would favor a deformation mode that involves a sub-lithostatic downdip pressure gradient in the channel, i.e., a downdip increase of pressure in the solid matrix that is less than the increase of overburden with depth. This compaction and flow-supported pressure gradient within the matrix can preferentially 'suck in' the lowest viscosity material from updip regions of the channel to replenish the

volume lost to fluid escape (Figure 6f). This effect, characteristic of flow in a region with strong lateral viscosity variations, would contribute to channel deformation by adding a dynamic downdip Poiseuille flow and pressure component to shear flow and to density-induced pressure variations (Figure 6g).

[72] The only place where we have multiple penetrations through the toe of an erosive margin is off-shore Costa Rica [Kimura *et al.*, 1997; Morris *et al.*, 2003]. Here, the thickness of the SC was found to increase by roughly one order of magnitude downdip near the surface inlet of the channel [Maltman and Vannucchi, 2004] (Figure 5). (Note this observed flow pattern directly implies a less than overburden pressure gradient within the solid matrix of this inlet portion of the channel!) If deeper parts of the channel are supplied through the inlet, then, to conserve mass, here the flow of material at the inlet exceeds the plate velocity (Figure 6a). An implication of this parabolic flow velocity profile is that there should be two zones of maximum shear, one at the channel's top, the other at its base, with a shear velocity inversion near the channel's base. If fluids focus where deformation is most intense, then fluids would concentrate in the zones of maximum strainrate found at the top and bottom of a region with a strong Poiseuille flow component. An inversion of shear sense was documented below the 'channel-bottom' surface of maximum shear in the Costa Rica plate boundary during ODP Leg 205 [Morris *et al.*, 2003]. It needs to be observationally verified in other locations whether or not near inlet broadening of the SC and an inversion of shear sense near the base of the inlet are in general features of erosive SCs — with a corresponding need to see if dynamic channel models can reproduce this mode of two-phase deformation where dynamic deformation concentrates within the weak channel in preference to increased deformation of the stronger overlying forearc and underlying subducting plate.

[73] Volume conservation in a dewatering channel can also be achieved by adding new material to the channel by eroding material from its upper (or lower) boundary. In this case subduction erosion would be the preferred tectonic process occurring along subduction plate boundaries, e.g., a typical instead of exceptional subduction process. This is seen in global syntheses of subduction accretion and subduction erosion [von Huene and Scholl, 1991; Clift and Vannucchi, 2004].

[74] Fluids also produce deformation and permeability variations through hydrofracturing and other modes of fluid-rock interaction. More work is needed to better understand these modes of coupled fluid/

rock migration/deformation [Phipps Morgan and Holtzman, 2005; Kohlstedt and Holtzman, 2009].

[75] Finally, this revised picture of SC processes has significant implications for future attempts to quantitatively model the SC/forearc system. In erosion, especially, there will be changes in the material properties of the overlying forearc. Changes in permeability of the forearc would influence the ability of fluids to 'leak' from the channel, especially in the upper parts of the SC. The SC is likely to be a dynamic 'boundary condition' at the base of a deforming forearc, influencing the forearc with its erosive aspects and fluid injection, while at the same time being influenced by the forearc's (time-dependent?) ability to effectively drain, or not drain, deeper parts of the channel, and to supply material into a compacting, deforming, channel.

Acknowledgments

[76] The authors thank Kelin Wang, Christie Rowe, and the associate editor for helpful advice. This work was supported by MIUR (PRIN 2008TWE5CX).

References

- Bachmann, R., J. Glodny, O. Oncken, and W. Seifert (2009a), Abandonment of the South Penninic-Austroalpine palaeo-subduction zone, Central Alps, and shift from subduction erosion to accretion: Constraints from Rb/Sr geochronology, *J. Geol. Soc.*, *166*, 217–231, doi:10.1144/0016-76492008-024.
- Bachmann, R., O. Oncken, J. Glodny, W. Seifert, V. Georgieva, and M. Sudo (2009b), Exposed plate interface in the European Alps reveals fabric styles and gradients related to an ancient seismogenic coupling zone, *J. Geophys. Res.*, *114*, B05402, doi:10.1029/2008JB005927.
- Bangs, N. L., T. H. Shipley, S. P. S. Gulick, G. F. Moore, S. Kuromoto, and Y. Nakamura (2004a), Evolution of the Nankai Trough decollement from the trench into the seismogenic zone: Inferences from three-dimensional seismic reflection imaging, *Geology*, *32*, 273–276, doi:10.1130/G20211.2.
- Bangs, N. L., T. H. Shipley, S. P. S. Gulick, G. F. Moore, S. Kuromoto, and Y. Nakamura (2004b), Evolution of the Nankai Trough decollement from the trench into the seismogenic zone: Inferences from three-dimensional seismic reflection imaging, *Geology*, *32*(4), 273–276, doi:10.1130/G20211.2.
- Bangs, N. L. B., G. F. Moore, S. P. S. Gulick, E. M. Pangborn, H. J. Tobin, S. Kuramoto, and A. Taira (2009), Broad, weak regions of the Nankai Megathrust and implications for shallow coseismic slip, *Earth Planet. Sci. Lett.*, *284*(1–2), 44–49, doi:10.1016/j.epsl.2009.04.026.
- Bolton, A. J., P. Vannucchi, B. Clennell, and A. J. Maltman (2000), Microstructural and geomechanical constraints on fluid flow at the Costa Rica convergent margin, ODP Leg 170 [online], *Proc. Ocean Drill Program Sci. Results*, *170*, 32 pp. [Available at http://www-odp.tamu.edu/publications/170_SR/VOLUME/CHAPTERS/SR170_03.PDF.]
- Calahorra, A. B., V. Sallares, J. Y. Collot, F. Sage, and C. R. Ranero (2008), Nonlinear variations of the physical

- properties along the southern Ecuador subduction channel: Results from depth-migrated seismic data, *Earth Planet. Sci. Lett.*, 267(3–4), 453–467, doi:10.1016/j.epsl.2007.11.061.
- Chamot-Rooke, N., et al. (1992), Tectonic context of fluid venting at the toe of the Eastern Nankai accretionary prism: Evidence for a shallow detachment fault, *Earth Planet. Sci. Lett.*, 109(3–4), 319–332, doi:10.1016/0012-821X(92)90095-D.
- Chan, L. H., and M. Kastner (2000), Lithium isotopic compositions of pore fluids and sediments in the Costa Rica subduction zone: Implications for fluid processes and sediment contribution to the arc volcanoes, *Earth Planet. Sci. Lett.*, 183(1–2), 275–290, doi:10.1016/S0012-821X(00)00275-2.
- Chopin, C. (1984), Coesite and pure pyrope in high-grade blueschists of the western Alps—a first record and some consequences, *Contrib. Mineral. Petrol.*, 86, 107–118, doi:10.1007/BF00381838.
- Chopin, C. (2003), Ultrahigh-pressure metamorphism: Tracing continental crust into the mantle, *Earth Planet. Sci. Lett.*, 212(1–2), 1–14, doi:10.1016/S0012-821X(03)00261-9.
- Clift, P., and P. Vannucchi (2004), Controls on tectonic accretion versus erosion in subduction zones: Implications for the origin and recycling of the continental crust, *Rev. Geophys.*, 42, RG2001, doi:10.1029/2003RG000127.
- Clift, P. D., I. Pecher, N. Kukowski, and A. Hampel (2003), Tectonic erosion of the Peruvian forearc, Lima Basin, by subduction and Nazca Ridge collision, *Tectonics*, 22(3), 1023, doi:10.1029/2002TC001386.
- Cloos, M., and R. L. Shreve (1988a), Subduction-channel model of prism accretion, mélange formation, sediment subduction, and subduction erosion at convergent plate margins: 1. background and description, *Pure Appl. Geophys.*, 128(3–4), 455–500, doi:10.1007/BF00874548.
- Cloos, M., and R. L. Shreve (1988b), Subduction-channel model of prism accretion, mélange formation, sediment subduction, and subduction erosion at convergent plate margins: 2. Implications and discussion, *Pure Appl. Geophys.*, 128(3–4), 501–545, doi:10.1007/BF00874549.
- Cloos, M., and R. L. Shreve (1996), Shear-zone thickness and the seismicity of Chilean- and Marianas-type subduction zones, *Geology*, 24(2), 107–110, doi:10.1130/0091-7613(1996)024<0107:SZTATS>2.3.CO;2.
- Collot, J.-Y., S. Lallemand, B. Pelletier, J. P. Eissen, G. Glaçon, M. A. Fisher, H. G. Greene, J. Boulain, J. Daniel, and M. Monzier (1992), Geology of the D'Entrecasteaux–New Hebrides arc collision zone: Results from a deep submersible survey, *Tectonophysics*, 212(3–4), 213–241, doi:10.1016/0040-1951(92)90292-E.
- Collot, J.-Y., W. Agudelo, A. Ribodetti, and B. Marcaillou (2008a), Origin of a crustal splay fault and its relation to the seismogenic zone and underplating at the erosional north Ecuador-south Colombia oceanic margin, *J. Geophys. Res.*, 113, B12102, doi:10.1029/2008JB005691.
- Collot, J.-Y., A. Ribodetti, B. Marcaillou, and W. Agudelo (2008b), Coeval subduction erosion and underplating associated with a crustal splay fault at the Ecuador-Colombia convergent margin, paper presented at 7th International Symposium on Andean Geodynamics, Inst. de Rech. pour le Dev., Nice, France, 2–4 Sept.
- Collot, J.-Y., A. Ribodetti, W. Agudelo, and F. Sage (2010), Where is the subduction fault?: Insights from a PSDM seismic line across the Ecuador convergent margin, *Geophys. Res. Abstracts*, 12, EGU2010-9982.
- Collot, J. Y., A. Ribodetti, W. Agudelo, and F. Sage (2011), The South Ecuador subduction channel: Evidence for a dynamic mega-shear zone from 2D fine-scale seismic reflection imaging and implications for material transfer, *J. Geophys. Res.*, 116, B11102, doi:10.1029/2011JB008429.
- Currie, C. A., K. Wang, R. D. Hyndman, and J. H. He (2004), The thermal effects of steady-state slab-driven mantle flow above a subducting plate: The Cascadia subduction zone and backarc, *Earth Planet. Sci. Lett.*, 223(1–2), 35–48, doi:10.1016/j.epsl.2004.04.020.
- Dahlen, F. A., J. Suppe, and D. Davis (1984), Mechanics of fold-and-thrust belts and accretionary wedges: Cohesive Coulomb theory, *J. Geophys. Res.*, 89, 10,087–10,101, doi:10.1029/JB089iB12p10087.
- Davis, D., J. Suppe, and F. A. Dahlen (1983), Mechanics of fold-and-thrust belts and accretionary wedges, *J. Geophys. Res.*, 88, 1153–1172, doi:10.1029/JB088iB02p01153.
- Dominguez, S., S. E. Lallemand, J. Malavieille, and R. von Huene (1998), Upper plate deformation associated with seamount subduction, *Tectonophysics*, 293(3–4), 207–224, doi:10.1016/S0040-1951(98)00086-9.
- Dominguez, S., J. Malavieille, and S. E. Lallemand (2000), Deformation of accretionary wedges in response to seamount subduction: Insights from sandbox experiments, *Tectonics*, 19(1), 182–196, doi:10.1029/1999TC900055.
- Eberhart-Phillips, D., and M. Reyners (1999), Plate interface properties in the northeast Hikurangi subduction zone, New Zealand, from converted seismic waves, *Geophys. Res. Lett.*, 26, 2565–2568, doi:10.1029/1999GL900567.
- England, P. C., and T. J. B. Holland (1979), Archimedes and the Tauern eclogites: The role of buoyancy in the preservation of exotic eclogite blocks, *Earth Planet. Sci. Lett.*, 44, 287–294, doi:10.1016/0012-821X(79)90177-8.
- Erickson, S. N., and R. D. Jarrard (1998), Velocity-porosity relationships for water-saturated siliciclastic sediments, *J. Geophys. Res.*, 103(B12), 30,385–30,406.
- Ernst, W. G. (2006), Preservation/exhumation of ultrahigh-pressure subduction complexes, *Lithos*, 92(3–4), 321–335, doi:10.1016/j.lithos.2006.03.049.
- Fagereng, A., and S. Ellis (2009), On factors controlling the depth of interseismic coupling on the Hikurangi subduction interface, New Zealand, *Earth Planet. Sci. Lett.*, 278(1–2), 120–130, doi:10.1016/j.epsl.2008.11.033.
- Fagereng, A., and R. H. Sibson (2010), Melange rheology and seismic style, *Geology*, 38(8), 751–754, doi:10.1130/G30868.1.
- Fagereng, A., F. Remitti, and R. H. Sibson (2010), Shear veins observed within anisotropic fabric at high angles to the maximum compressive stress, *Nat. Geosci.*, 3(7), 482–485, doi:10.1038/ngeo898.
- Federico, L., L. Crispini, M. Scambelluri, and G. Capponi (2007), Ophiolite melange zone records exhumation in a fossil subduction channel, *Geology*, 35(6), 499–502, doi:10.1130/G23190A.1.
- Fisher, D. M., and T. Byrne (1987), Structural evolution of underthrust sediments, Kodiak Island, Alaska, *Tectonics*, 6, 775–793, doi:10.1029/TC006i006p00775.
- Gerya, T. V., and B. Stockhert (2002), Exhumation rates of high pressure metamorphic rocks in subduction channels: The effect of rheology, *Geophys. Res. Lett.*, 29(8), 1261, doi:10.1029/2001GL014307.
- Grevenmeyer, I., et al. (2004), Fluid flow through active mud Dome Mound Culebra offshore Nicoya Peninsula, Costa Rica: Evidence from heat flow surveying, *Mar. Geol.*, 207(1–4), 145–157, doi:10.1016/j.margeo.2004.04.002.
- Gutscher, M. A., N. Kukowski, J. Malavieille, and S. Lallemand (1998), Episodic imbricate thrusting and underthrusting: Analog experiments and mechanical analysis applied to

- the Alaskan accretionary wedge, *J. Geophys. Res.*, **103**, 10,161–10,176, doi:10.1029/97JB03541.
- Hampel, A., N. Kukowsky, J. Bialas, C. Huebscher, and R. Heinbockel (2004), Ridge subduction at an erosive margin: Collision zone of the Nazca Ridge in Southern Peru, *J. Geophys. Res.*, **109**, B02101, doi:10.1029/2003JB002593.
- Harris, R. N., G. Spinelli, C. R. Ranero, I. Grevenmeyer, H. Villinger, and U. Barckhausen (2010a), The thermal regime of the Costa Rican convergent margin: 2. Thermal models of the shallow Middle America Subduction Zone offshore Costa Rica, *Geochem. Geophys. Geosyst.*, **11**, Q12S29, doi:10.1029/2010GC003273.
- Harris, R. N., I. Grevenmeyer, C. R. Ranero, H. Villinger, U. Barckhausen, T. Henke, C. Muller, and S. Neben (2010b), The thermal regime of the Costa Rican convergent margin: 1. Along strike variations in heat flow from probe measurements and estimated from bottom simulating reflectors, *Geochem. Geophys. Geosyst.*, **11**, Q12S28, doi:10.1029/2010GC003272.
- Hashimoto, Y., and G. Kimura (1999), Underplating process from melange formation to duplexing: Example from the Cretaceous Shimanto Belt, Kii Peninsula, southwest Japan, *Tectonics*, **18**(1), 92–107, doi:10.1029/1998TC900014.
- Henry, P., S. Lallemand, K. Nakamura, U. Tsunogai, S. Mazzotti, and K. Kobayashi (2002), Surface expression of fluid venting at the toe of the Nankai wedge and implications for flow paths, *Mar. Geol.*, **187**, 119–143, doi:10.1016/S0025-3227(02)00262-1.
- Hensen, C., K. Wallmann, M. Schmidt, C. R. Ranero, and E. Suess (2004), Fluid expulsion related to mud extrusion off Costa Rica—A window to the subducting slab, *Geology*, **32**(3), 201–204, doi:10.1130/G20119.1.
- Hoffman, N. W., and H. J. Tobin (2004), An empirical relationship between velocity and porosity for underthrust sediments in the Nankai Trough accretionary prism, *Proc. Ocean Drill. Program Sci. Results*, **190/196**, 1–23, doi:10.2973/odp.proc.sr.190196.190355.192004.
- Housen, B. A., et al. (1996), Strain decoupling across the decollement of the Barbados accretionary prism, *Geology*, **24**(2), 127–130, doi:10.1130/0091-7613(1996)024<0127:SDATDO>2.3.CO;2.
- Hyndman, R. D., M. Yamano, and D. A. Oleskevich (1997), The seismogenic zone of subduction thrust faults, *Isl. Arc*, **6**(3), 244–260, doi:10.1111/j.1440-1738.1997.tb00175.x.
- Ikesawa, E., G. Kimura, K. Sato, K. Ikehara-Ohmori, Y. Kitamura, A. Yamaguchi, K. Ujiie, and Y. Hashimoto (2005), Tectonic incorporation of the upper part of oceanic crust to overriding plate of a convergent margin: An example from the Cretaceous-early Tertiary Mugli Melange, the Shimanto Belt, Japan, *Tectonophysics*, **401**(3–4), 217–230, doi:10.1016/j.tecto.2005.01.005.
- Karner, S. L., F. M. Chester, A. K. Kronenberg, and J. S. Chester (2003), Subcritical compaction and yielding of granular quartz sand, *Tectonophysics*, **377**, 357–381, doi:10.1016/j.tecto.2003.10.006.
- Kawabata, K., H. Tanaka, Y. Kitamura, and K. F. Ma (2009), Apparent activation energy and rate-limiting process estimation from natural shale deformed by pressure solution in shallow subduction zone, *Earth Planet. Sci. Lett.*, **287**(1–2), 57–63, doi:10.1016/j.epsl.2009.07.032.
- Kawamura, K., Y. Ogawa, R. Anma, S. Yokoyama, S. Kawakami, Y. Dilek, G. F. Moore, S. Hirano, A. Yamaguchi, and T. Sasaki (2009), Structural architecture and active deformation of the Nankai Accretionary Prism, Japan: Submersible survey results from the Tenryu Submarine Canyon, *Geol. Soc. Am. Bull.*, **121**(11–12), 1629–1646, doi:10.1130/B26219.1.
- Kimura, G., E. A. Silver, and P. Blum, and the ODP Leg 170 Shipboard Scientific Party (1997), *Proceedings of the Ocean Drilling Program, Initial Reports*, vol. 170, 458 pp., Ocean Drill. Program, College Station, Tex.
- Kimura, G., G. F. Moore, M. Strasser, E. Screaton, D. Curewitz, C. Streiff, and H. Tobin (2011), Spatial and temporal evolution of the megasplay fault in the Nankai Trough, *Geochem. Geophys. Geosyst.*, **12**, Q0A008, doi:10.1029/2010GC003335.
- Kitamura, Y., et al. (2005), Mélange and its seismogenic roof décollement: A plate boundary fault rock in the subduction zone—An example from the Shimanto Belt, Japan, *Tectonics*, **24**, TC5012, doi:10.1029/2004TC001635.
- Klaeschen, D., I. Belykh, H. Gribidenko, S. Patrikeyev, and R. von Huene (1994), Structure of the Kuril trench from seismic reflection records, *J. Geophys. Res.*, **99**(B12), 24,173–24,188, doi:10.1029/94JB01186.
- Kohlstedt, D. L., and B. K. Holtzman (2009), Shearing melt out of the Earth: An experimentalist's perspective on the influence of deformation on melt extraction, *Annu. Rev. Earth Planet. Sci.*, **37**, 561–593, doi:10.1146/annurev.earth.031208.100104.
- Kondo, H., G. Kimura, M. Hideki, K. Ohmori-Ikehara, Y. Kitamura, E. Ikesawa, A. Sakaguchi, A. Yamaguchi, and S. Okamoto (2005), Deformation and fluid flow of a major out-of-sequence thrust located at seismogenic depth in an accretionary complex: Nobeoka Thrust in the Shimanto Belt, Kyushu, Japan, *Tectonics*, **24**, TC6008, doi:10.1029/2004TC001655.
- Labaume, P., M. Kastner, A. Trave, and P. Henry (1997), Carbonate veins from the décollement zone at the toe of the Northern Barbados accretionary prism: Microstructure, mineralogy, geochemistry and relations with prism structures and fluid regime, *Proc. Ocean Drill. Program Sci. Result*, **156**, 79–96.
- Le Pichon, X., et al. (1992), Fluid venting activity within the Eastern Nankai trough accretionary wedge: A summary of the 1989 Kaiko-Nankai results, *Earth Planet. Sci. Lett.*, **109**(3–4), 303–318, doi:10.1016/0012-821X(92)90094-C.
- Le Pichon, X., S. Lallemand, M. Fournier, J. P. Cadet, and K. Kobayashi (1994), Shear partitioning in the Eastern Nankai Trough: Evidence from submersible dives, *Earth Planet. Sci. Lett.*, **128**(3–4), 77–83, doi:10.1016/0012-821X(94)90136-8.
- Maltman, A. J., and P. Vannucchi (2004), Insights from the Ocean Drilling Program on shear and fluid-flow at the mega-faults between actively converging plates, in *Flow Processes in Faults and Shear Zones*, edited by G. I. Alsop et al., *Geol. Soc. Spec. Publ.*, **224**, 127–140, doi:10.1144/GSL.SP.2004.224.01.09.
- Mancktelow, N. S. (1995), Nonlithostatic pressure during sediment subduction and the development and exhumation of high-pressure metamorphic rocks, *J. Geophys. Res.*, **100**(B1), 571–583, doi:10.1029/94JB02158.
- Marcaillou, B., G. Spence, K. Wang, J. Y. Collot, and A. Ribodetti (2008), Thermal segmentation along the N. Ecuador–S. Colombia margin (1–4°N): Prominent influence of sedimentation rate in the trench, *Earth Planet. Sci. Lett.*, **272**(1–2), 296–308, doi:10.1016/j.epsl.2008.04.049.
- McIntosh, K., E. Silver, and T. Shipley (1993), Evidence and mechanisms for fore-arc extension at the accretionary Costa Rica Convergent Margin, *Tectonics*, **12**(6), 1380–1392, doi:10.1029/93TC01792.
- Meneghini, F., G. Di Toro, C. D. Rowe, J. C. Moore, A. Tsutsumi, and A. Yamaguchi (2010), Record of mega-earthquakes in subduction thrusts: The black fault rocks of Pasagshak Point, *Geol. Soc. Am. Bull.*, **122**(7–8), 1280–1297, doi:10.1130/B30049.1.

- Micklethwaite, S., and S. F. Cox (2006), Progressive fault triggering and fluid flow in aftershock domains: Examples from mineralized Archean fault systems, *Earth Planet. Sci. Lett.*, **250**, 318–330, doi:10.1016/j.epsl.2006.07.050.
- Mishra, O. P., and D. P. Zhao (2003), Crack density, saturation rate and porosity at the 2001 Bhuj, India, earthquake hypocenter: A fluid-driven earthquake?, *Earth Planet. Sci. Lett.*, **212**(3–4), 393–405, doi:10.1016/S0012-821X(03)00285-1.
- Moore, D. E., and D. A. Lockner (2004), Crystallographic controls on the frictional behavior of dry and water-saturated sheet structure minerals, *J. Geophys. Res.*, **109**, B03401, doi:10.1029/2003JB002582.
- Moore, J. C., and T. Byrne (1987), Thickening of fault zones: A mechanism of melange formation in accreting sediments, *Geology*, **15**, 1040–1043, doi:10.1130/0091-7613(1987)15<1040:TOFZAM>2.0.CO;2.
- Moore, J. C., and D. Saffer (2001), Updip limit of the seismogenic zone beneath the accretionary prism of southwest Japan: An effect of diagenetic to low-grade metamorphic processes and increasing effective stress, *Geology*, **29**(2), 183–186, doi:10.1130/0091-7613(2001)029<0183:ULOTSZ>2.0.CO;2.
- Moore, J. C., and P. Vrolijk (1992), Fluids in accretionary prisms, *Rev. Geophys.*, **30**, 113–135, doi:10.1029/92RG00201.
- Moore, J. C., et al. (1995), Abnormal fluid pressures and fault-zone dilation in the Barbados accretionary prism: Evidence from logging while drilling, *Geology*, **23**(7), 605–608, doi:10.1130/0091-7613(1995)023<0605:AFPAFZ>2.3.CO;2.
- Morgan, J. P., and D. E. Karig (1994), The estimation of diffuse strains in the toe of the western Nankai accretionary prism: A kinematic solution, *J. Geophys. Res.*, **99**(B4), 7019–7032, doi:10.1029/93JB03367.
- Morris, J. D., H. W. Villinger, and A. Klaus, and the ODP Leg 205 Shipboard Scientific Party (2003), *Proceedings of the Ocean Drilling Program, Initial Reports* [CD-ROM], **205**, 75 pp., Ocean Drill. Program, College Station, Tex.
- Nedimović, M. R., R. D. Hyndman, K. Ramachandran, and G. D. Spence (2003), Reflection signature of seismic and aseismic slip on the northern Cascadia subduction interface, *Nature*, **424**(6947), 416–420, doi:10.1038/nature01840.
- Newman, A. V., S. Y. Schwartz, V. Gonzalez, H. R. DeShon, J. M. Protti, and L. M. Dorman (2002), Along-strike variability in the seismogenic zone below Nicoya Peninsula, Costa Rica, *Geophys. Res. Lett.*, **29**(20), 1977, doi:10.1029/2002GL015409.
- Nur, A., G. Mavko, J. Dvorkin, and D. Galmudi (1998), Critical porosity: A key to relating physical properties to porosity in rocks, *Leading Edge*, **17**(3), 357–362, doi:10.1190/1.1437977.
- Obana, K., S. Kodaira, Y. Kaneda, K. Mochizuki, M. Shinohara, and K. Suyehiro (2003), Microseismicity at the seaward updip limit of the western Nankai Trough seismogenic zone, *J. Geophys. Res.*, **108**(B10), 2459, doi:10.1029/2002JB002370.
- Okamoto, S., G. Kimura, and H. Yamaguchi (2006), Earthquake fault rock including a coupled lubrication mechanism, *eEarth Discuss.*, **1**, 135–149.
- Oleskevich, D. A., R. D. Hyndman, and K. Wang (1999), The updip and downdip limits to great subduction earthquakes: Thermal and structural models of Cascadia, south Alaska, SW Japan, and Chile, *J. Geophys. Res.*, **104**, 14,965–14,991, doi:10.1029/1999JB900060.
- Park, J. O., T. Tsuru, S. Kodaira, P. R. Cummins, and Y. Kaneda (2002), Splay fault branching along the Nankai subduction zone, *Science*, **297**(5584), 1157–1160, doi:10.1126/science.1074111.
- Phipps Morgan, J., and B. K. Holtzman (2005), Vug waves: A mechanism for coupled rock deformation and fluid migration, *Geochem. Geophys. Geosyst.*, **6**, Q08002, doi:10.1029/2004GC000818.
- Pytte, A. M., and R. C. Reynolds (1989), The thermal transformation of smectite to illite, in *Thermal History of Sedimentary Basins: Methods and Case Histories*, edited by N. D. Naeser and T. H. McCulloh, pp. 133–140, Springer, New York, doi:10.1007/978-1-4612-3492-0_8.
- Raimbourg, H., and G. Kimura (2008), Non-lithostatic pressure in subduction zones, *Earth Planet. Sci. Lett.*, **274**(3–4), 414–422, doi:10.1016/j.epsl.2008.07.037.
- Raimbourg, H., Y. Hamano, S. Saito, M. Kinoshita, and A. Kopf (2011), Acoustic and mechanical properties of Nankai accretionary prism core samples, *Geochem. Geophys. Geosyst.*, **12**, Q0AD10, doi:10.1029/2010GC003169.
- Ramsay, J. G. (1980), The crack-seal mechanism of rock deformation, *Nature*, **284**, 135–139, doi:10.1038/284135a0.
- Ranero, C. R., and R. von Huene (2000), Subduction erosion along the Middle America convergent margin, *Nature*, **404**, 748–752, doi:10.1038/35008046.
- Ranero, C. R., I. Grevemeyer, U. Sahling, U. Barckhausen, C. Hensen, K. Wallmann, W. Weinrebe, P. Vannucchi, R. von Huene, and K. McIntosh (2008), The hydrogeological system of erosional convergent margins and its influence on tectonics and interplate seismogenesis, *Geochem. Geophys. Geosyst.*, **9**, Q03S04, doi:10.1029/2007GC001679.
- Remitti, F., P. Vannucchi, G. Bettelli, L. Fantoni, F. Panini, and P. Vescovi (2011), Tectonic and sedimentary evolution of the frontal part of an ancient subduction complex at the transition from accretion to erosion: The case of the Ligurian wedge of the northern Apennines, Italy, *Geol. Soc. Am. Bull.*, **123**(1–2), 51–70, doi:10.1130/B30065.1.
- Ribodetti, A., S. Operto, W. Agudelo, J.-Y. Collot, and J. Virieux (2011), Joint ray + Born least-squares migration and simulated annealing optimization for high-resolution target-oriented quantitative seismic imaging, *Geophysics*, **76**, R23–R42, doi:10.1190/1.3554330.
- Rupke, L. H., J. Phipps Morgan, M. Hort, and J. A. D. Connolly (2004), Serpentine and the subduction zone water cycle, *Earth Planet. Sci. Lett.*, **223**(1–2), 17–34, doi:10.1016/j.epsl.2004.04.018.
- Saffer, D. M. (2003), Pore pressure development and progressive dewatering in underthrust sediments at the Costa Rican subduction margin: Comparison with northern Barbados and Nankai, *J. Geophys. Res.*, **108**(B5), 2261, doi:10.1029/2002JB001787.
- Saffer, D. M., and B. A. Bekins (1998), Episodic fluid flow in the Nankai accretionary complex: Timescale, geochemistry, flow rates, and fluid budget, *J. Geophys. Res.*, **103**(B12), 30,351–30,370, doi:10.1029/98JB01983.
- Sage, F., J. Y. Collot, and C. R. Ranero (2006), Interplate patchiness and subduction-erosion mechanisms: Evidence from depth-migrated seismic images at the central Ecuador convergent margin, *Geology*, **34**(12), 997–1000, doi:10.1130/G22790A.1.
- Scherwath, M., et al. (2010), Fore-arc deformation and underplating at the northern Hikurangi margin, New Zealand, *J. Geophys. Res.*, **115**, B06408, doi:10.1029/2009JB006645.
- Scholz, C. H. (1998), Earthquakes and friction laws, *Nature*, **391**, 37–42, doi:10.1038/34097.
- Screaton, E. J., and D. M. Saffer (2005), Fluid Expulsion and overpressure development during initial subduction at the Costa Rica convergent margin, *Earth Planet. Sci. Lett.*, **233**, 361–374, doi:10.1016/j.epsl.2005.02.017.
- Secor, D. T. (1965), Role of fluid pressure in jointing, *Am. J. Sci.*, **263**, 633–646, doi:10.2475/ajs.263.8.633.

- Shreve, R. L., and M. Cloos (1986), Dynamics of sediment subduction, melange formation, and prism accretion, *J. Geophys. Res.*, **91**(B10), 10,229–10,245, doi:10.1029/JB091iB10p10229.
- Sibson, R. H. (2000), A brittle failure mode plot defining conditions for high-flux flow, *Econ. Geol.*, **95**, 41–48, doi:10.2113/gsecongeo.95.1.41.
- Sibson, R. H. (2001), Seismogenic framework for hydrothermal transport and ore deposition, *Rev. Econ. Geol.*, **14**, 25–50.
- Sibson, R. H., and J. V. Rowland (2003), Stress, fluid pressure and structural permeability in seismogenic crust, North Island, New Zealand, *Geophys. J. Int.*, **154**(2), 584–594, doi:10.1046/j.1365-246X.2003.01965.x.
- Silver, E., M. Kastner, A. Fisher, J. Morris, K. McIntosh, and D. Saffer (2000), Fluid flow paths in the Middle America Trench and Costa Rica margin, *Geology*, **28**(8), 679–682, doi:10.1130/0091-7613(2000)28<679:FFPITM>2.0.CO;2.
- Strasser, M., et al. (2009), Origin and evolution of a splay fault in the Nankai accretionary wedge, *Nat. Geosci.*, **2**, 648–652, doi:10.1038/ngeo609.
- Tobin, H. J., and D. M. Saffer (2009), Elevated fluid pressure and extreme mechanical weakness of a plate boundary megathrust, Nankai Trough subduction zone, *Geology*, **37**, 679–682, doi:10.1130/G25752A.1.
- Townend, J. (1997), Subducting a sponge; minimum estimates of the fluid budget of the Hikurangi Margin accretionary prism, *Geol. Soc. N. Z. News.*, **112**, 14–16.
- Tsuji, T., H. Tokuyama, P. C. Pisani, and G. Moore (2008), Effective stress and pore pressure in the Nankai accretionary prism off the Muroto Peninsula, southwestern Japan, *J. Geophys. Res.*, **113**, B11401, doi:10.1029/2007JB005002.
- Tsuru, T., J.-O. Park, S. Miura, S. Kodaira, Y. Kido, and T. Hayashi (2002), Along-arc structural variation of the plate boundary at the Japan Trench margin: Implication of interplate coupling, *J. Geophys. Res.*, **107**(B12), 2357, doi:10.1029/2001JB001664.
- Ujiié, K., H. Yamaguchi, A. Sakaguchi, and S. Toh (2007), Pseudotachylytes in an ancient accretionary complex and implications for melt lubrication during subduction zone earthquakes, *J. Struct. Geol.*, **29**(4), 599–613, doi:10.1016/j.jsg.2006.10.012.
- Vannucchi, P., and L. Leoni (2007), Structural characterization of the Costa Rica decollement: Evidence for seismically induced fluid pulsing, *Earth Planet. Sci. Lett.*, **262**, 413–428, doi:10.1016/j.epsl.2007.07.056.
- Vannucchi, P., C. R. Ranero, S. Galeotti, S. M. Straub, D. W. Scholl, and K. McDougall-Ried (2003), Fast rates of subduction erosion along the Costa Rica Pacific margin: Implications for nonsteady rates of crustal recycling at subduction zones, *J. Geophys. Res.*, **108**(B11), 2511, doi:10.1029/2002JB002207.
- Vannucchi, P., F. Remitti, and G. Bettelli (2008), Geological record of fluid flow and seismogenesis along an erosive subducting plate boundary, *Nature*, **451**, 699–703, doi:10.1038/nature06486.
- Vannucchi, P., F. Remitti, J. Phipps Morgan, and G. Bettelli (2009), The aseismic-seismic transition and fluid regime along subduction plate boundaries and a fossil example from the Northern Apennines of Italy, in *Fault-Zone Properties and Rupture Dynamics*, *Int. Geophys. Ser.*, vol. 94, edited by E. Fukuyama, pp. 37–68, Elsevier, Burlington, Mass.
- Vannucchi, P., F. Remitti, G. Bettelli, C. Boschi, and L. Dallai (2010), Fluid history related to the early Eocene-middle Miocene convergent system of the Northern Apennines (Italy): Constraints from structural and isotopic studies, *J. Geophys. Res.*, **115**, B05405, doi:10.1029/2009JB006590.
- von Huene, R., and S. Lallemand (1990), Tectonic erosion along the Japan and Peru convergent margins, *Geol. Soc. Am. Bull.*, **102**(6), 704–720, doi:10.1130/0016-7606(1990)102<0704:TEATJA>2.3.CO;2.
- von Huene, R., and C. R. Ranero (2003), Subduction erosion and basal friction along the sediment-starved convergent margin off Antofagasta, Chile, *J. Geophys. Res.*, **108**(B2), 2079, doi:10.1029/2001JB001569.
- von Huene, R., and D. W. Scholl (1991), Observations at convergent margins concerning sediment subduction, subduction erosion, and the growth of continental crust, *Rev. Geophys.*, **29**(3), 279–316, doi:10.1029/91RG00969.
- von Huene, R., C. R. Ranero, W. Weinrebe, and K. Hinz (2000), Quaternary convergent margin tectonics of Costa Rica, segmentation of the Cocos Plate, and Central American volcanism, *Tectonics*, **19**(2), 314–334, doi:10.1029/1999TC001143.
- von Huene, R., C. R. Ranero, and P. Vannucchi (2004), Generic model of subduction erosion, *Geology*, **32**(10), 913–916, doi:10.1130/G20563.1.
- Wallace, L. M., et al. (2009), Characterizing the seismogenic zone of a major plate boundary subduction thrust: Hikurangi Margin, New Zealand, *Geochem. Geophys. Geosyst.*, **10**, Q10006, doi:10.1029/2009GC002610.
- Wang, K. (2010), Finding fault in fault zones, *Science*, **329**, 152–153, doi:10.1126/science.1192223.
- Wang, K. L., and Y. Hu (2006), Accretionary prisms in subduction earthquake cycles: The theory of dynamic Coulomb wedge, *J. Geophys. Res.*, **111**, B06410, doi:10.1029/2005JB004094.
- Wang, K. L., Y. Hu, R. von Huene, and N. Kukowski (2010), Interplate earthquakes as a driver of shallow subduction erosion, *Geology*, **38**(5), 431–434, doi:10.1130/G30597.1.
- Wong, T. F., C. David, and W. L. Zhu (1997), The transition from brittle faulting to cataclastic flow in porous sandstones: Mechanical deformation, *J. Geophys. Res.*, **102**, 3009–3025, doi:10.1029/96JB03281.